ON-LINE MONITORING DURING EXTRUSION COOKING OF AN EXPANDED CEREAL SNACK

by

LEAH RACHEL MILLER

(Under the Direction of Jake H. Mulligan)

ABSTRACT

On-line monitoring devices are fast and precise tools that enable characterization of materials during processing. Raman spectroscopy and non-destructive ultrasound techniques were utilized on-line during extrusion cooking of a cereal snack in this study. The objectives were to determine the effects of extrusion variables on final properties, determine the type of chemical bonds present during extrusion, and to establish a relationship between on-line monitoring tools and textural properties of an extrudate. The results showed that temperature and formulation have significant effects on color values as well as hardness, crispness, and brittleness of the product. Common Raman bands found during extrusion were indicators of bonding in starch, protein, and lipids; many of these chemical bonds withstood high levels of shear but not temperatures above 90°C. The data displayed that attenuation from non-destructive ultrasound is a good predictor for the texture variables hardness and brittleness ($P < 0.05$).

INDEX WORDS: Extrusion, cereal, on-line process monitoring, Raman, non-destructive ultrasound, texture

ON-LINE MONITORING DURING EXTRUSION COOKING OF AN EXPANDED CEREAL SNACK

by

LEAH RACHEL MILLER

B.S., Virginia Polytechnic Institute and State University, 2007

A Thesis Submitted to the Graduate Faculty of The University of Georgia in Partial Fulfillment of the Requirements for the Degree

MASTER OF SCIENCE

ATHENS, GEORGIA

2009

ON-LINE MONITORING DURING EXTRUSION COOKING OF AN EXPANDED CEREAL SNACK

by

LEAH RACHEL MILLER

Major Professor:	Jake H. Mulligan
Committee:	Mark A. Harrison
	Robert L. Shewfelt
	Rakesh K. Singh

Electronic Version Approved:

Maureen Grasso
Dean of the Graduate School
The University of Georgia
August 2009

DEDICATION

I would like to dedicate this work to my family, David, Becky, and Megan for all of their love, support, and never-ending encouragement without which this would not have been possible. Also to the 32 from whom I have obtained the inspiration and heart to never give up.

ACKNOWLEDGEMENTS

I would like to thank Dr. Mulligan, Dr. Harrison, Dr. Shewfelt, and Dr. Singh for all of the guidance they have given and effort put towards helping me achieve my master's degree. I would also like to acknowledge all those that have taken part in this project: George Cavender, Danny Morris, Phodchanee (Tina) Phongpa-ngan, Amudhan Ponrajan, Puranjay Priyadarshi, Carl Ruiz, and Darlene Samuel.

TABLE OF CONTENTS

LIST OF TABLES

Page

LIST OF FIGURES

Page

CHAPTER 1

INTRODUCTION

Production of cereal-based snack foods has been on the rise for the last 20 years and continues to grow in popularity. An estimated total of $20.69 billion was spent on snack foods in 2000 averaging a 6% increase per year (Maga 2000). As the demand for cereal snacks grows, the food industry continues to find ways to increase production and efficiency while decreasing waste. In the past, processing of these snacks was performed by traditional batch methods that included mixing, forming, baking and drying. The amount of waste produced was not only exorbitant but the required energy to fuel the equipment and time necessary can greatly hindered a company's profitability. Cereal snack processing has been revolutionized by the utilization of extrusion cooking. Twin-screw extrusion is able to decrease space, costs, overall waste, and encumbers several steps from conventional processing into one device (Maga 1991). While extrusion is a vast improvement from the previous processing methods, perfecting the operation of its several parameters (screw speed, temperature, feed rate, feed moisture) to obtain a consistently desired product quality is still lagging.

In order to understand the uniqueness of each parameter along with its effect on the final product's textural properties the inclusion of on-line monitoring has been approached (Grenier and Bellon-Maurel 2003). Currently the majority of on-line monitoring is being used to detect contaminants in foods whether it be microbial or physical but new technologies have greatly advanced available tools. On-line monitoring allows the operator to receive information on the physicochemical properties of a material while still undergoing the effects of processing. For the detection of structural changes such as bond formations, Raman spectroscopy is the leading technique to be used as an on-line evaluation. This type of vibrational spectroscopy functions off

of backscattering as a near infrared incident beam excites molecular bonds in the components of a food material (Smith and Dent 2005). With the bonding information received from a Raman spectrum an understanding of the food's chemical nature can be established. In addition to the chemical properties, non-destructive ultrasound is an effective means to acquiring data on the physical characteristics of a food product. As a sound wave is sent and received back as a function of reflectance, the deciphered velocity and amplitude changes will provide information on the density variations throughout the process.

To help further understand, as precisely as possible, what effect these physicochemical characteristics of a food material have on the final textural properties a study was conducted. The third chapter describes the effect of extrusion parameters on the physical and textural attributes of a cereal-based snack. The fourth chapter addresses how the structural and physical nature of an extrudate were monitored during extrusion and how these characteristics relate to the final textural properties.

References

Grenier, P., Bellon-Maurel, V., 2003. Using spectroscopic techniques to monitor food composition. In I.E. Tothill (Ed.), Rapid and on-line instrumentation for food quality assurance. CRC Press LLC, Boca Raton, pp. 291-305.

Maga, J.A., 1991. Cereal-Based Snack Foods. In K.J. Lorenz, K. Kulp (Eds.), Handbook of Cereal Science and Technology. Marcel Dekker, Inc., New York, pp. 793-814.

Maga, J.A., 2000. Handbook of Cereal Science and Technology. In K.J. Lorenz, K. Kulp (Eds.), Cereal-based Snack foods. CRC Press, Manhattan.

Smith, E., Dent, G., 2005. Modern Raman Spectroscopy - A Practical Approach. John Wiley & Sons, Ltd, West Sussex, England.

CHAPTER 2

LITERATURE REVIEW

Introduction to Cereals

Cereals are the most abundant food worldwide and supply more energy in the diet than any other crop. They are grown for their edible portions, the bran, germ and endosperm that provide basic nutritional needs. The concept of cereals encumbers a multitude of crops grown in various places around the globe. The most highly demanded of the cereals is maize, followed by rice, wheat and barley; the less notable yet still present cereals produced are triticale, oats, quinoa, millet, rye, sorghum, buckwheat, and fonio (Friedman 1996).

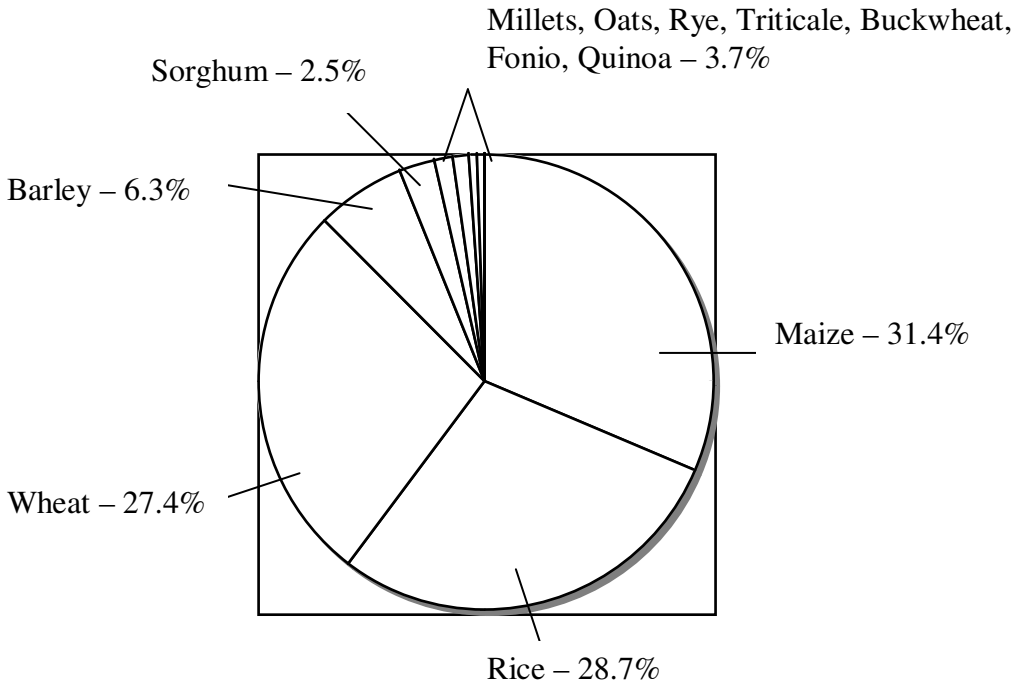

Figure 2.1. 2006 Cereals production (Maga 2000)

According to Johnson (1991) the only continent that is not a producer of maize is Antarctica while the United States remains at the top. The corn kernel is the biggest seed of all the cereals

with the largest fraction composed of the endosperm. Currently the utilization of corn has endless possibilities from popcorn to alcohol, sweeteners, starches, and flours. Rice tends to have more limited contributions to the food industry, mostly present in its original form but often used for brewing beer, cereals, soups and is a vital portion of the diet in most of Asia. As the rice crop has evolved, so has the amount of cultivars produced throughout the world, now at a staggering 100,000 (Sharp 1991). When compared to wheat classes, currently at seven, the magnitude of this number is even more apparent. Wheat, however, is a constituent of more foods worldwide than any other cereal grain and also tends to have a higher concentration of vitamins. As the last significant cereal produced, barley is best known for its contribution to the beer industry; the malting of this grain gives beer its distinct flavor and aroma. The use of barley in beer often overshadows its consumption by other means all of which have decreased over the last century because of difficulties incorporating the grain into food materials (Kent and Evers 1994).

Nutrient Composition of Cereals

There are three vital components to cereals that make their production and consumption an invaluable part of everyday life: proteins, lipids, and carbohydrates. For each type of cereal grain the concentration of these macronutrients is different throughout which is a common concern when excessive processing of the grain takes place. In order to evaluate the overall nutritional value without incorporating losses during milling, rolling, and other processing only the whole grain will be addressed. Protein's function in a cereal grain is to provide enough amino acids necessary to obtain proper nutrition. There are a total of 22 amino acids and, with their difference in structure and length, supply very diverse nutritional value. Plant proteins, in general, are broken down into categories of water soluble (albumins), saline soluble (globulins),

aqueous alcohol soluble (prolamins), and insoluble (Evers et al. 1999). Following is a table of the major cereal grains and their storage proteins:

Table 2.1. Storage proteins in cereal grains (Maga 1991)

Cereal Grain	Protein
Maize	prolamin (zein)
Rice	glutelins (oryzenin)
Wheat	gliadin, glutenin (gluten)
Barley	prolamins (hordeins), glutelins

As the second type of macronutrient in cereals, lipids are normally found in the germ portion of the whole grain and can be in a variety of forms. Fatty acids are a primary form of lipids in cereals and consist of a long hydrocarbon chain linked to a carboxylic acid group. Fatty acids can be saturated, unsaturated, or polyunsaturated and this bonding status greatly influences their nutritional value for the consumer; unsaturated fatty acids dominate the cereal grain lipid composition (Chung 1991). Glycerides, often known as acylglycerols, are normally stored as tri-acylglycerols in plants meaning there are three fatty acids attached to a glycerol molecule. These tend to be the most common type of lipid that is removed during processing. Fat-soluble vitamins A, D, E, and K are also present in small amounts in whole grains.

Lastly, carbohydrate compounds tend to receive the most attention in that they make up the largest portion of the cereal grain. Carbohydrates are classified by the degree of polymerization, from monosaccharides to oligosaccharides, and the largest, polysaccharides. Monosaccharides combine to form disaccharides by a glycosidic link, with one sugar molecule having a free reducing group available for interactions. Sucrose displays this type of bonding

between glucose and fructose and is prominent during the early stages of the cereal grain before being converted to starch and other carbohydrates during the mature cycle. Starch is composed of polysaccharides (glucans) as is cellulose but with different glycosidic linkages. Because cellulose (a component of dietary fiber) contains a β-linkage as opposed to an α-link it is indigestible by the human gastrointestinal tract and is seen less often in foods than starch. Starch is the most prevalent of all carbohydrates and outweighs others with its utilization in food systems and extensive functionality (Evers et al. 1999).

Functionality of Starch

The most abundantly found carbohydrate in all cereal grains, next to cellulose, is starch which comprises 60 to 70% of the dry matter. Starch is one of the primary sources of energy for humans and animals and is often utilized for the functional properties it can impart upon food. It can be used a thickening agent for sauces and gravies, a stabilizer for salad dressings, a gel-forming agent, and as many other roles including aiding in digestion (BeMiller and Whistler 1996). These applications all depend on the composition of starch and how the environment affects its granular structure. Starch is a highly ordered granule with birefringence in the shape of a maltese cross. It is composed of two macromolecules amylose and amylopectin. Amylose is the smaller of the two molecules, with a molecular weight of $1.6x10^5$ to $7.1x10^5$ and is made up of linear chained α-1,4-linked glucose molecules (from 50-2000 glucose units). While there may be few α-1,6 branches throughout, the other macromolecule in starch, amylopectin, contains multiple branches off of a short-chained α-1,4-linked glucose molecules and has a much larger molecular weight of 10^8 (17-26 glucose residues) (Collado and Corke 2003).

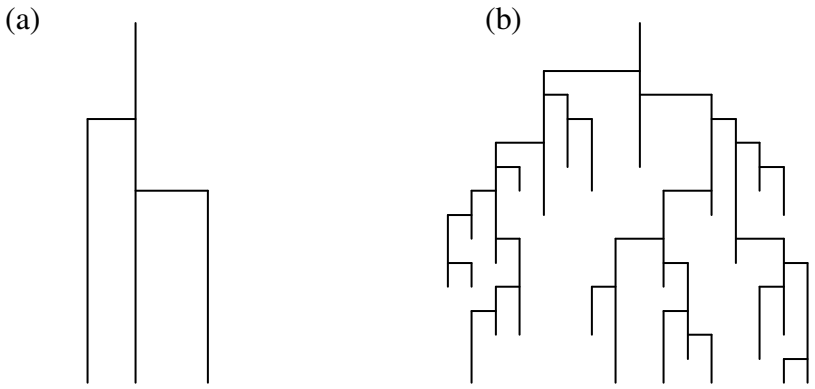

Figure 2.2. Components of starch: (a) amylose and (b) amylopectin (Colonna et al. 1989)

Due to the longer chain, amylose has the ability to change its structure by becoming helical within solution if hydrogen bonding occurs with the hydroxyl groups; this allows the connection with alcohols, organic acids, and often lipids (Evers et al. 1999). Amylopectin, however, is more resistant to the chemical and physical modifications starch undergoes causing amylose to be most often disturbed. Gelatinization occurs in starch when the right conditions are present. Heating at 60-70°C and a large enough water concentration causes a crystalline state to become amorphous. In this endothermic process, the starch granule takes up water, swells, and becomes a disordered state. Amylopectin concentration remains the same within the granule. However, amylose leaches out both during and after gelatinization, so while the viscosity of the discontinuous phase increases from swelling, the continuous gel phase is now composed of a three-dimensional amylose network (Hermansson and Svegmark 1996).

The strength of this formed starch gel is dependent on the volume fraction of the dispersed phase of swollen granules in the continuous phase of amylose that has leached out of the system and has become entangled in water. As starch gels are held or cooled, hydrogen bonding can occur between the free amylose molecules causing a crystallization known as

retrogradation. Retrogradation is understood as the reassociation of molecules within starch to form an aggregated, insoluble complex from what was a disordered system (Colonna et al. 1989). This process can be both an advantageous and disastrous step in food production but most often causes syneresis of gels and hardening of baked goods (Evers et al. 1999). The ability to control the modifications of starch can greatly influence the textural properties and nutritional value of a food product.

Cereal Processing

Incorporating cereals into snack-like products is not a new concept, especially in the United States which leads the world in highest consumption. The table below shows the magnitude of the American consumers' habits with snack food:

Table 2.2. 1991 Snack foods consumption and cost in the U.S. (Maga 1991)

Year	Billion Spent ($)	Billion Consumed (lbs)
1990	12.72	4.62
1991	13.43	4.92
1992	13.80	5.18
1993	14.66	5.52
1994	15.05	5.69
1995	15.09	5.54
1996	15.32	5.57
1997	16.44	5.73

Because it is such a large market there are many factors taken into consideration when producing a successful snack. Attributes such as overall flavor, texture, and appearance are a huge motivation when buying a cereal snack; these are highly dependent on the shelf-life and

nutritional value of the food material which is, in turn, a feature of how the food was processed. It is known that high temperatures, low pH, and long time treatments often degrade vitamins, polysaccharides, and other essential nutrients from the grain and this is after proper milling and rolling techniques have taken place. Other contributors to nutrient degradation and decreased shelf-life in cereal-based foods are light, oxygen, increased water activity, metals, and the activity of enzymes (Ranhotra 1991). The inactivation of enzymes is an essential step in cereal processing as it can yield a product with all of the positive attributes and prevents complete degradation by unfolding the enzyme and inactivating its center. Lipase is a common enzyme found in grains that breaks down triglycerides and releases free fatty acids; other lipid-associated enzymes, peroxidase and lipoxygenase, act in different ways and result in decreased stability. (Bookwalter et al. 1991) found that, using peroxidase as the model enzyme as it is the most resistant to processing effects, these lipid-attacking enzymes can be inactivated at processing temperatures of 91°C or higher for twelve minutes. Significant inactivation of lipase is also possible in a forced draft oven at 175°C for 15 to 30 minutes due to the dry heat utilization (Rose et al. 2008). Often present in cereal grains are proteolytic enzymes that act to degrade proteins by cleavage of peptide bonds connecting amino acids. The effectiveness of these enzymes depends on what type of protein is being attacked and if the processing parameters used are powerful enough to degrade a portion of their activity. One of the most common enzymes in cereal grains, amylase, functions by breaking down starch into sugar molecules but is similar to proteolytic enzymes in that it is efficiently inactivated by the process of extrusion (van der Veen et al. 2004). With conventional processing, high temperatures and low moisture contents can aid in the degradation of these enzymes while adding a high shear environment maximizes the results. Extrusion cooking of cereals in not beneficial for solely inactivation of enzymes but also for high

productivity, energy efficiency, continuous processing while maintaining product quality, and its high degree of versatility between ingredients and products.

Extrusion of Cereals

Extrusion has been a common practice in the food industry and continues to grow in applicability especially in preparing starch-based snack foods. It is a high temperature, short time process that runs on a continuous basis and is capable of manufacturing a vast array of foodstuffs. One of the greatest attractions of extrusion is its ability to encompass several conventional methods into one instrument with the addition of high shear forces (Balasubramanian and Singh 2007). In an extruder there are several sections vital to product quality: feeding, conveying, kneading, forming, and pressuring. The extent of product modification depends on the extruder itself. There are several types of available extruders with twin-screw extruders being the most often utilized and is what was operated in this study. This form of extrusion allows for more versatility, high efficiency, ability to incorporate a variety of ingredients, pressure balance and a large throughput (Vessa 1990).

Within the twin-screw extruder there are different types of screw configurations and geometries such as co-rotating, counter-rotating, intermeshing and non-intermeshing. The co-rotating, intermeshing twin-screw extruder is used most often in the food industry due to enhanced characteristics and performance ability. This screw configuration employs a self-wiping capability as the flight of one screw is engaged in the channel of the other. Each screw can be assembled as to the operator's liking depending on the type of raw materials and desired outcome; altering the pitch, or distance between each flight. By choosing different types of screws, one can greatly alter the final product. Throughout sections of the extruder kneading

blocks are often added to increase mixing, shear, and energy distribution by either a backward or forward flow (Harper 1989).

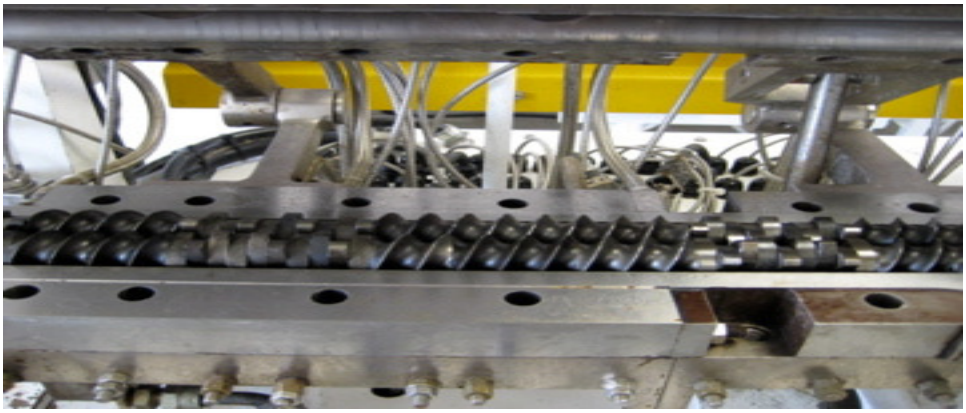

Figure 2.3: Twin-screw, co-rotating, intermeshing extruder configuration

Kneading block thickness aids in the control of mixing that can occur during extrusion; narrower blocks tend to cause a distributive mixing whereas dispersive mixing can be achieved with wide kneading blocks. Because twin-screw extruders have high mixing capabilities, the use of viscous, sticky, high moisture raw materials does not hinder the extrusion process (Senanayake and Clarke 1999).

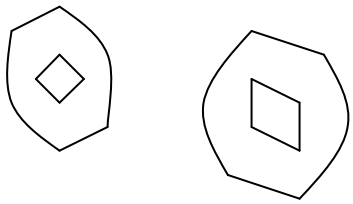

Figure 2.4: Kneading blocks

Other components of the extruder also have an effect on final product quality: the feed hopper by which the mass flow rate of raw materials is established, a jacketed barrel that either heats or cools the dough, the water pump to alter moisture content, and the die at which the

product is pressurized, shaped, and exits. Within each portion of the extruder are controllable parameters vital to producing a successful extrudate by optimizing the influence on physical and sensory attributes (Liu et al. 2000). The solid feed rate (kg/h) determines the amount of raw materials conveyed into the extruder barrel from the feed hopper over a specified amount of time. This factor can determine the output, shear levels, amount of necessary energy, and also the final product quality if used in conjunction with screw speeds (RPM) (Altomare and Ghossi 1986). The screws, in general, determine the capacity of an extruder due to their diameter, pitch and flights however, the actual screw speeds have a larger effect on the system. Residence time, or the amount of time it takes a particle to go through the entire barrel, is dependent on the screw speed and will furthermore effect the degree of cooking on the dough; lower screw speeds, a larger pitch, more length, will all lead to a longer residence time (Martelli 1967). Screw speeds alter the amount of shear that either increases or decreases the viscosity of the material by changing the bonding characteristics as will be discussed later.

Another independent variable, feed moisture (%), is added to the barrel in order to achieve the desired final moisture content. The moisture in the system is largely dependent on the barrel temperature and determines the final temperature of the extrudate once it leaves the die; lower moisture content dough will be hotter than a higher moisture dough after being subjected to the same degree of heat (Altomare and Ghossi 1986). This temperature control throughout the barrel is one of the key features in affecting bonding characteristics to form the appropriate product. In addition, the barrel itself must be able to withstand immense amount pressure and shear without wearing down. Within the barrel wall, temperatures are set, normally going from low to high moving down the barrel to the die. This gives the feed time to enter the barrel, be introduced to water, and effectively encounter high amounts of shear and temperature

to cook, mix, and form the foodstuff before exiting the extruder. There are also often increases in temperature due to friction that can add to cooking the material.

During the extrusion process, the raw materials are subjected to high pressures with the apex at the die entrance. It is here that stagnation flow can occur, leading to burning and degradation of the material if the die is not shaped correctly. A conical flow will help the material flow uniformly while also placing focus on the ratio of length to the cross sectional area of the die hole where the product is shaped. A shorter length to diameter ratio contributes to increase swelling of the extrudate; swelling occurs due to the rapid change in pressure (from high to atmospheric) and, in turn, the flashing off of moisture as steam.

Swelling of the extrudate is largely dependent on the type of bonding that has occurred throughout the extrusion process due to chemical transformations. As the dough proceeds down the extruder, the bonding characteristics are directly proportion to the levels of shear and temperature. Starch, a vital component to raw materials, is a viscoelastic material and can undergo extensive conversions due to extruder conditions. The breakdown of starch to low molecular weight macromolecules occurs from the splitting of hydrogen bonds, giving water room to move in and causing the starch to become more soluble; what once was amylose and amylopectin is now degraded into small chains of molecules (Apruzzese et al. 2000). Depending on the initial ratio of amylose to amylopectin along with the previously described variables, the crystalline structure of starch can be completely destroyed as well as its granular properties (Colonna et al. 1989). To fully understand the degradation of starch it is important to study the kinetics of starch reactions resulting from thermal and mechanical forces as depicted from this equation:

$$k = f(\tau, \gamma, \eta, T, M, \dots) \quad (1)$$

where τ and γ are the shear stress and shear rate, η, the viscosity of the materials, T, the extrusion temperature and M, the moisture content of starch (Zheng and Wang 1994). Using this equation in conjunction with others focusing on rate constants and activation energies, Zheng and others (1994) conducted a study on the extrusion of waxy corn starch. They found that the degree of starch conversion depends more on shear levels than the barrel temperature during processing but together can be extremely detrimental to the starch structure. These factors can increase the internal energy of starch molecules enough to allow for high degrees of molecular movement yielding melting and degradation.

Just as starch undergoes changes during extrusion, structural changes occur to native proteins attributable to both shear and temperature. Bonds that form the tertiary and quaternary structure of protein are broken leading to a denaturation of the molecule. As proteins unfold down the barrel, they also begin to orient with other protein molecules and form linkages to stabilize the dough structure.

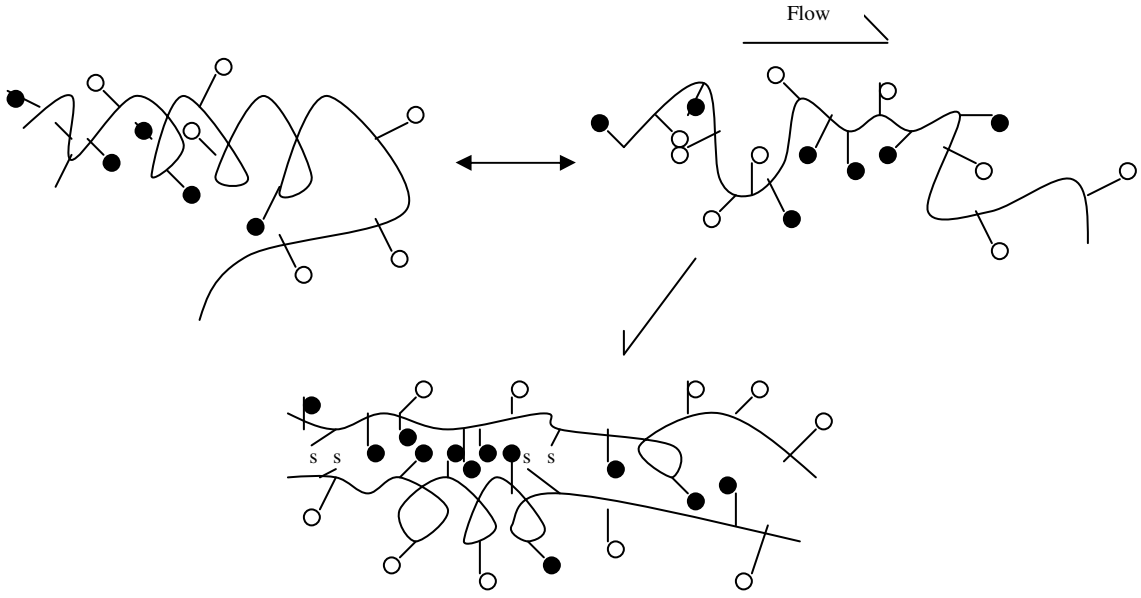

Figure 2.5: Protein denaturation during extrusion cooking (Camire 1991)

Amino acid residues slowly become exposed, such as tyrosine and phenylalanine, and allow other hydrophobic molecules to attach themselves (Camire 1991). Covalent bonding that cross-links protein molecules together plays an important role in establishing the final product's characteristics. Disulfide type of cross-linking formed from cysteine residues and hydrophobic and electrostatic interactions has been shown to decrease throughout extrusion, especially when there is a significant increase in temperature. When the bonds are broken, free sulfhydryl groups are given off and have been shown in large concentration at the end of the barrel before exiting the die (Hager 1984).

Nondisulfide bonds are attributable to three possible interactions: isopeptides, Maillard products, and intermolecular cross-links. With the data from Jeunink and others (1979), the latter type of bonding plays the least significant role in texturization of proteins if any and has yet to be further investigated. The Maillard reaction, due to ε-amino groups bonding with a reducing sugar, has not been extensively studied by extrusion but the change in color along with decreased protein nutritional quality gives some insight that it is a possible cause of cross-linking. Isopeptides formation is concluded to be the primary factor for nondisulfide bonds as it is quantifiable by the presence or absence of specific amino acids. This cross-linking is greatly influential for protein texturization and overall physical properties of the extrudate (Stanley 1989). Protein interactions during extrusion is such a vague topic so in order to better understand the mechanics, more research is being done to actively monitor the cooking process and its affect on protein molecules. Sampling the raw materials beforehand and the cooked product is not enough when trying to determine the physicochemical changes the macromolecule undergoes. Because it is often assumed that protein aggregation and cross-linking takes place at the die, studying the process more closely will give a clearer insight as to at what point during extrusion

will have the greatest effect on the protein structural changes and how to control it (Della Valle et al. 1994).

Researchers have found that protein denaturation and furthermore cross-linking occurs at the highest rate during low moisture, low screw speed, and low temperature extrusion. A longer residence time and a potential for increased thermal degradation of the proteins will undoubtedly be detrimental to a protein system. When this occurs at such a fast rate, the final product is likely to be more compact with less expansion and a higher density. This is often an undesirable characteristic for the ready-to-eat foods associated with extrusion so levels of protein within ingredient formulations must be established based on each individual product.

Effect of Extrusion Parameters on Final Product

While it is understood that individual parameters able to be controlled on the extruder have an overall effect on the raw material, it is more important to understand the intricacies of these characteristics on its final textural attributes. The three main properties of an extrudate affected by extrusion conditions are density, expansion ratio, and overall textural characteristics; expansion can be broken down into the viscosity and die swell of the dough and only takes into account the expansion perpendicular to the flow (Harmann and Harper 1973). Ingredient formulation is the first factor considered when attempting to extrude and has the capability to influence the entire process and outcome.

First, the amount of starch present in the raw materials alters the degree of gelatinization and ultimately the rheological characteristics of the cooked dough. With a decreased amylose to amylopectin ratio, there will be a much larger expansion ratio but with a high concentration of starch, the density will increase, aiding in expansion. Protein tends to have the opposite affect on

extrudates, yielding a much denser, less expanded product at certain additions. This is one of the disadvantageous to extruding high protein ready-to-eat foods and therefore the processing conditions must be tweaked correctly to alter the structure of proteins for a desirable product. The case is similar for high-fiber products, a sought-after concept yet one not quite perfectly attainable through extrusion. Fiber has been shown to decrease expansion leaving a harder texture by not allowing gas bubbles to fully expand when flashing off moisture. The lower expansion creates a very compact extrudate that often has a layer of "shark skin" which is undesirable to both the operator and consumer. Shark skin replaces a smooth texture on the outer side of the product with jagged edges created as it exits the die. This occurs as the surface layer expands quicker than the other portions but cannot withstand the cell extensibility and therefore collapses. Lipids are often incorporated into feed materials for both the mouthfeel and emulsification capabilities. Lipids tend to reduce the friction within the barrel, creating a lower shear environment and decrease in degradation of starch molecules. When both starch and lipids are present within the extruder, an insoluble amylose-lipid complex can be formed and gives a lower viscosity dough with a higher expansion (Colonna and Mercier 1983). The details of this interaction is limited as little has been done to evaluate changes throughout extrusion.

As the raw materials are introduced to water via a pump, the amount of water added can effectively alter the extrudate final properties. Feed moisture has the greatest effect on both the density and expansion of the material compared to other variables. A direct relationship is seen with feed moisture and density and indirect with expansion, attributable to slight viscosity changes and, in turn, pressure differences (Singh et al. 2007). This association leads to conclusions that feed moisture controls much of starch gelatinization during extrusion which has a major correlation with physical properties (Ding et al. 2006). Decreased gelatinization of starch

molecules, decreased elasticity, combined with the inability of thin cell walls to withstand the high amount of steam flashing off creates a smaller, denser foodstuff (Faubion and Hoseney 1982). Stojceska and others (2009) found that feed moisture also significantly contributes to protein content resulting in a decrease as moisture increases.

Color, while being a significant result of raw materials, is also somewhat dependent on the amount of moisture in the dough. As moisture percentage increases, the product will generate a darker color because of a lighter thermal treatment. Additionally, altering the moisture content at specified screw speeds can either increase or decrease the shear strength and manipulate the structural properties of the dough. Shear level is a function of screw speed making the RPM a significant factor in texture. Higher screw speeds result in lower density cooked material because of the decrease in viscosity of the dough and increased elasticity characteristics as reported by Fletcher et al. (1985). Even though it decreases residence time, screw speeds between 200-300 RPM have also been shown to degrade both protein and starch molecules allowing for more water incorporation and a low density extrudate with higher expansion (Guha et al. 1997).

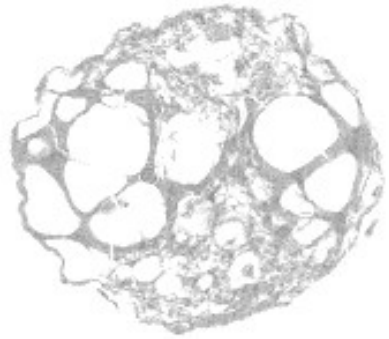

Figure 2.6: MicroCT image of a highly expanded cereal snack

As the screw speed increases, the temperature due to friction increases while the barrel temperature is still placing heat on the product. This constant barrel temperature aids in heating

the water to give way to a phase transition that decreases the melt viscosity and density. The higher the barrel temperature prior to exiting the die, the greater expansion will be present, creating a more aerated product (Fletcher et al. 1985).

The density and expansion of food products are directly related to their textural properties as often established using texture analyzers. Cereal products formed by extrusion must maintain a certain level of hardness and crispness in order to be acceptable to the consumer. Both characteristics are related to how the product responds when under stress and can be distinguished by mimicking the reaction of the mouth. The hardness of a cereal product describes the ability of the food to resist breaking when subjected to a high amount of force; crispness is better understood as the breaking of the snack due to force involving an identifiable sound (Jowitt 1974). Brittleness is also often used to describe an extrudate and exemplifies a product that fractures after only a small distance of force has been applied. When applying these terms to extrusion, they best correlate with the expansion of an extrudate along with its air dispersion and cellular structure which are influenced by extrusion parameters. If the feed moisture of the dough is increased, the product will yield a much harder texture especially if used in conjunction with a high feed rate. As was identified before, amplified screw speed aids in the expansion and decreased density of a food material and can furthermore decrease the hardness. Because of the incorporation of air, the necessary energy to puncture said extrudate is reduced, making it less hard (Ding et al. 2006). Overall high temperatures of the raw materials throughout the barrel, from both set values and friction, result in similar textural products of increase screw speeds, decreased hardness and brittleness.

On-line Process Monitoring

When extruding a product the majority of the work, and also the primary issue, is concerned with correct processing parameters and how they will then affect the extrudate. Current manufacturing practices only perform post-processing evaluations on the extrudate once most has been extruded which often leads to large amounts of waste. If it is necessary to process a specific amount of material in order to get a representative sample for testing, the loss in both time and cost can be detrimental. In order to alleviate this problem, the concept of on-line monitoring during the process must be approached. Employing an on-line monitoring system would give the operator capabilities that were never feasible before but also those that could alter the performance of an entire line. Traditional methods have been used but are often time consuming and detrimental to the product quality which has lead to a new era of non-destructive, rapid techniques.

Raman spectroscopy can be added as an on-line monitoring tool in almost any setting and will formulate an in-depth knowledge of the product at each step. With new technology it is now a portable, easy to use, straightforward method and can offer the highly specific information about the material's components and their individual molecular structures. As information is read from the screen attached to the equipment, an understanding of the bonds breaking and forming within the material and the structural differences that will occur in the final product is formulated. While the initial costs of acquiring a Raman spectrometer may be high, the long-term benefits of using this on-line system may be worth it. This is also the case with a non-destructive ultrasound system in which rapid, noninvasive, and precise measurements can be taken all throughout the process. There are several ultrasonic properties that can be related to physical properties of the food material, enabling the operator to better anticipate the final

characteristics. Through the use of low frequency acoustic waves and a system capable of converting an electric signal into an ultrasonic signal, ultrasound is becoming a more desired technique of continuously monitoring a food process. These mechanisms of on-line processing will enhance product quality, reduce the amount of waste, and increase the efficiency while keeping control of the process.

Raman Spectroscopy

Utilization of Raman spectroscopy as an on-line monitoring tool is not common but has the ability to characterize the structural forms of a substance, also often referred to as fingerprinting. In providing a qualitative understanding of the examined samples the components are able to be identified as well as quantitatively measured. Raman spectroscopy uses visible or near-infrared light as the excitation source. On-line process monitoring does not always allow for the transmittance of light due to both materials and equipment; near-infrared light Raman spectroscopy works off of backscattering therefore the density of the sample and the type of equipment being used is not an interference. In addition, the sample being examined can be opaque as opposed to the often-necessary clear sample which further emphasizes the usefulness of Raman as a on-line monitoring tool.

A major disadvantage to visible Raman spectroscopy is the occurrence of fluorescence in the region governed by Stokes scattering and that can, in turn, result in inaccurate signals (Freeman 1974). This is likely a factor in the analysis of organic compounds but this technique is capable of detection in a vast array of materials including solids, liquids, and gaseous samples at a wide range of temperatures. An advantage of Raman spectroscopy is the capability of determining molecular structures in aqueous solutions. The weakness of water and other polar

groups in this technique are overshadowed by the intensity of nonpolar groups such as S-S and C=C that show up vividly in the spectrum (Ma and Phillips 2002). The ability to use aqueous systems in this detection is essential for biological systems ranging from human tissue to food materials.

Table 2.3: Comparison of spectroscopic techniques (Freeman 1974)

Technique	Min Sample Size (g)	Aqueous Solutions	Finger-print	Quant. Analysis	Subtle Structural Features	General Analysis	Commercial Availability Of Ref. Spectra	Approx. Instrum Cost ($)
Raman	10^{-6}	very simple	excellent	good	good	excellent	poor	15,000 - 25,000
Infrared	10^{-6}	difficult	excellent	good	good	excellent	excellent	7,000 - 15,000
Proton NMR	$2x10^{-5}$	very simple	fair	good	excellent	excellent	fair	20,000
Mass	10^{-10}	difficult	good	poor	poor	good	good	40,000
UV	10^{-6}	very simple	poor	excellent	poor	poor	excellent	5,000 - 12,000

The phenomenon of Raman spectroscopy arrived in 1928 by Sir C. V. Raman who used sunlight as the light source and other crude instrumentation but was later built upon with advancements in science (Ferraro and Nakamoto 1994). The Raman theory is based on the concept that when monochromatic light interacts with a material, some of the light is scattered while other photons may be absorbed. A majority of the scattered light will have the same energy as the incident beam because the electron clouds are distorted only slightly enough to produce an insignificant change in the photon frequency of scattering. This type of scattering is referred to as elastic scattering (Rayleigh scattering) and due to the lack of energy transference to the molecule no change in energy states occurs; Rayleigh scattered light also has the same color and frequency of the original light. When the incident beam does transfer energy to the molecule or the molecule to the scattered photon a change of energy occurs yielding Raman scattering, an

inelastic process. The portion of light that undergoes Raman scattering is only 1 in 10^7 photons so it is a weak process.

Raman scattering encompasses two forms of light scattering, Stokes and anti-Stokes. Stokes scattering occurs when a molecule absorbs energy, enters the virtual state (determined by the frequency of the incident beam), ends up in a vibrational state with higher energy than initially and leaves the photon with a longer wavelength than the incident photon. However, if anti-Stokes scattering takes place the emitted photon will initially be in a higher, excited state, enter into the virtual state, and then scatter to the ground vibrational state which results in a increase in energy of the photon (Smith and Dent 2005). The intensity of scatter that occurs is proportional to the concentration of analyte in a sample. Scattering is expressed as the shift in wavenumber (Δcm^{-1}) from the exciting radiation and will be plotted on a Raman spectrum as intensity versus Δcm^{-1} (Freeman 1974).

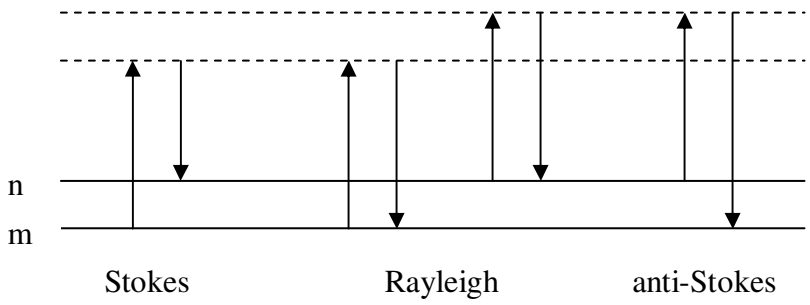

Figure 2.7: Rayleigh and Raman scattering energy shifts (Smith and Dent 2005)

The photons emitted from a molecule contain oscillating dipoles that are induced from the original light. The frequency at which the dipoles oscillate is dependent upon the direction of the force from the electric field and can be established by

$$\mu = \alpha E \qquad (2)$$

where μ is the dipole moment, E the electric field of the incident photon, and α is the polarizability of the molecule (Freeman 1974). The polarizability of a molecule is defined as the tendency of the electron cloud surrounding the molecule to be distorted by the said electric field. If the direction of the electric field vector (direction of force) is only vibrating in a single plane perpendicular to the propagation of the photons, the light is considered polarized; when the vector vibrates in all planes perpendicular then it is unpolarized light. For Raman scattered light, polarization of a molecule occurs when there is a shift in polarizability of the electron cloud due to the vibrations of the molecule from the incident light beam (Pelletier 1999). The scattered light polarization depends on whether the movement of the electron cloud is in the same direction as the polarization of light of the original beam. To ensure that the polarization of the incident photons remains the same through Raman spectroscopy detection, a polarizer is employed to establish a plane at which the light will be polarized (Smith and Dent 2005). Often an analyzer is present in the system to allow the polarized light to pass through the previously determined angle.

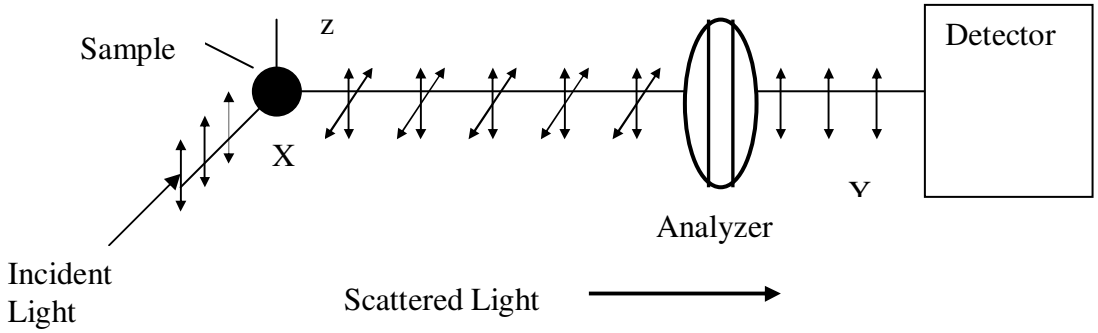

Figure 2.8: Monitoring polarization of light during Raman spectroscopy measurements (Smith and Dent 2005)

Two types of scattering arise from the change in polarization of scattered light: isotropic and anisotropic. Isotropic scattering occurs when the induced dipole moment, and analyzer, are

parallel to the driving electric field and always has a constant dipole moment regardless of the change of intensity of the electric field. Anistropic scattering from molecules results from a dipole moment perpendicular to the plane of the electric field (Stevenson and Vo-Dinh 1996). These Raman scattering movements have an effect on the Raman intensity, as does the number of molecules vibrating from the light and the intensity of the incident light beam. The vibration frequency of the molecules is controlled by the speed of light (c), force constant (k), and reduced mass (μ_r) of the two masses connected by the chemical bonds:

$$\omega = \frac{1}{2\pi r} \cdot \left(\frac{k}{\mu_r} \right)^{1/2} \qquad (3)$$

After deciphering Equation 3, it is determined that a triple bond has a higher vibrational frequency than a double bond and so on. Characteristic frequencies of specific bonds in molecules are reported in literature and can be used to analyze a Raman spectrum.

Raman Instrumentation

As stated previously, a monochromatic light source is used to excite the molecule, however in some cases this laser probe is attached to the spectrometer through a fibre optic cable. This allows for more versatility with the Raman equipment and encourages the use as an on-line monitoring tool. While the main function of the fibre optic cable is to transfer the light scattering to the main receiver, it often causes Raman scattering to occur within, altering the final recorded spectra. To aid in reducing these effects, the excitation source is produced through an inner channel and the emitted photons from the molecules are collected in a fiber separated by a filler but still located in the same cable (Pelletier 1999). The scattering of photons after excitation must then be controlled to eliminate Rayleigh scattering and allow Raman scattering to be

detected so there is no overlap of the weak emission. This is done with a multi-monochromater system that passes only the bands of interest through the instrument. The first separates the Raman scattering from Rayleigh scattering and the second greatly defines the different Raman peaks and their separate characteristics. Once the correct scattering has passed through the exit slit of the monochromator, a charge-coupled device (CCD) detector is utilized for its sensitivity to each frequency of scattered light. It is composed of silicon with two-dimensional arrays and is capable of decreasing the background noise and detecting photons over a wide range of wavelengths (Ferraro and Nakamoto 1994). The noise acquired during Raman analysis can greatly alter the Raman spectrum as can the Raman signal; the concept known as signal-to-noise ratio is useful in determining the quality of a Raman spectrum and is defined as the Raman intensity divided by the noise intensity. Certain components of the Raman instrument, such as the CCD as previously stated, aid in minimizing the noise factor and intensify the signal. Noise can be random, emphasizing the need to perform replicate measurements, or determinant and can be attributed to background light, the light emitted, and the instrumentation (Pelletier 1999). Understanding the possible contributors to noise and how that may affect the overall spectrum is essential in an accurate representation of a material.

Raman Spectra

Raman spectra exemplify the quality of a material by using peaks determined from the intensity and wavelength of the vibrational characteristics that are distinct for each component and the bonds within. Each peak within the Raman spectrum corresponds to a specific band of wavenumbers which is how the identification process takes place. Depending on the composition of the material being analyzed certain standard Raman spectrum can be used as reference

material. Protein, lipids, and carbohydrates are the major constituents of food systems and much focus is placed on them. The amino acids that form proteins are evaluated based on their interactions with one another and the side groups attached to the molecules. Often a Raman spectrum detects disulfide bonding, aromatic rings, charged functional groups, and peptide bonds. In cereal chemistry there are specific bands of proteins that are displayed: 400-500 cm^{-1} for disulfide bonds, 830-855 cm^{-1} for tyrosine linkages, a peak around 1350 cm^{-1} identifies with the indole ring of tryptophan, and several different amide bands are present in the 1200 and 1600 cm^{-1} ranges (Ikeda and Li-Chan 2004).

While not as prominent as protein scattering, the additions of lipids to a material also produces their own vibrational modes. Hydrocarbon chain interactions yield information on the type of packing and C=C stretching compared to C=O stretching exemplifies the degree of unsaturation of a molecule; these vibrational modes tend to give peaks in the 1400-1500 cm^{-1} region. Lipid interactions do not show up as clearly on a Raman spectrum so if detailed analyses of specific compounds are desired an alternative method should be used in conjunction with this vibrational spectroscopy (Li-Chan 1996).

Understanding carbohydrates in a food material is one of the most essential functions of a Raman spectrometer. Although there is little research on carbohydrates compared to other areas often utilizing Raman spectroscopy, determining the type of structural changes resulting from starch molecules and sugar will provide an in-depth interpretation of the material composition. Much of the importance surrounding carbohydrates has to do with starch and how its molecular alterations affect its functional properties; C-O-H vibrations from the amylose ratio of starch (1040 cm^{-1}) along with ring structures and side chains give some of the most distinct peaks. Carbohydrates known as disaccharides such as sucrose and glucose are identifiable through

Raman spectroscopy. Starch molecular vibrations give the most peaks in a Raman spectrum produced from a cereal-type product as shown below.

Table 2.4: Raman bands attributable to starch (Kizil et al. 2002)

Raman (cm^{-1})	Raman band assignment
440	skeletal modes of pyranose
783	C-C stretching
860	CH_2 deformation
936	skeletal mode vibrations of ∝-1,4 glycosidic linkage
1087	C-O-H bending
1122	C-O stretching, C-O-H bending
1260-1280	CH_2OH (side chain) related mode
1339	C-O-H bending, CH_2 twisting
1460	CH_2 bending
2800 – 3000	C-H stretching
3100 – 3500	O-H stretching

Non-destructive Ultrasound

The concept of ultrasound as a tool for analyzing food materials has been around for more than 60 years, but with the current push to find improved analytical techniques for evaluation it is now even more important to understand its worthiness. There have been many studies done on the applications of ultrasound with food systems from the detection of biscuit crispness (Povey and Harden 1981) to determining particles sizes of emulsions using velocity and attenuation (Howe et al. 1986). Ultrasound is used in two forms either low-intensity which is non-destructive or high-intensity which alters the physicochemical properties of a material; for the purpose of this study the former will be discusses. Low-intensity ultrasound uses a low

frequency acoustic wave to measure the interactions between sound and material (McClements 1995). Advantages to this type of ultrasound is, as stated, the non-destructive nature of the waves so no structural or chemical changes will occur throughout the foodstuff and also the ability to perform measurements on opaque foods. The sound wave most often used for in-line monitoring is called a longitudinal compressional wave because it is best with dense, complex materials (Povey and McClements 1988). This wave causes a displacement of particles, an oscillation, parallel to the direction of the sound as seen below

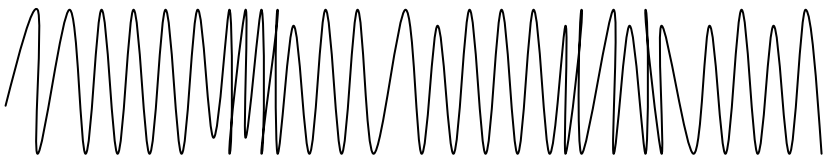

Figure 2.9: Longitudinal compressional wave used in an ultrasonic pulse-echo technique

It works by applying a stress wave to the surface of a material which causes the particles within to also oscillate. Energy from the wave can be transferred to the food as heat yet once the wave is reflected off, the energy fades and the layers go back to their original placement. The reflection of the wave off of the material is dependent upon its components and also in the shape of the surface, whether it be flat or curved, and therefore changes with the angle of the incidence wave and the acoustic impendances of all components. The acoustic impendance establishes how much of the sound wave will be reflected off of the surface instead of being absorbed:

$$Z = \frac{P}{U} = \frac{\omega\rho}{k} \qquad (4)$$

In Equation 3 the acoustic impendance (Z) is the ratio of the acoustic excess pressure (P) and the particle velocity (U) (McClements 1997).

The characteristics of this wave, as deciphered from an ultrasound signal, are plentiful and can then be used to establish properties of materials: amplitude (A), wavelength (λ), frequency (f), and attenuation coefficient (α). The amplitude of a wave is a measure of its intensity and changes between emission and receiving. The attenuation coefficient is also a factor based upon the material's composition as it is a measure of how quickly the amplitude decreases from the initial point to distance x (increase attenuation coefficient, increase rate of reduction). Attenuation coefficient can also be derived from the following equation

$$A = A_0 e^{-\alpha x} \tag{5}$$

wherein A_0 is the initial amplitude of the wave and x is the entire distance it has traveled through the food material. Attenuation coefficient is often expressed as Np/m and is normally high in doughs and batters so is often passed over for other properties. Ultrasonic velocity, or the distance traveled by a sound wave in a given time, is one of these evaluated characteristics that is used for solid materials with increased densities (Salazar et al. 2004). For high-attenuating materials it can be calculated using the wavelength at a specific frequency

$$c = \lambda f \tag{6}$$

The ultrasonic velocity does best at describing the G' (elastic modulus) and density of the material, with a greater influence on the former portion.

$$\frac{1}{c^2} = \frac{\rho}{E} \tag{7}$$

It can also help in monitoring phase transitions due to the fact that the velocity of an acoustic wave is greater in solids than liquids. Depending on the accessibility of information and necessary data, these properties can then be used to determine the real-time physicochemical properties of the material such as the composition and structure. This is done in two ways, either by empirical formulations or using a theoretical approach. The first way, empirically, uses

experimental data to find a best-fit equation for the data and then relate the properties of the wave to the true physical properties of the product. A disadvantage to this method is that it can only be used for simple, homogenous materials and can vary greatly due to random and determinant error. When the theoretical method is used, a greater knowledge of how each processing parameter affects the final product and how the sound wave interacts with the food is formed. It uses mathematical theories to relate ultrasonic properties to very intricate structural information about the material (McClements 1997).

Ultrasound Instrumentation

To produce a reliable ultrasound signal from which material properties are to be established, first the consideration of proper equipment must take place. There are many different variations to an ultrasound set-up but always contain a transducer, signal generator, digitizer, and a way to display the information. The signal generator sends the electrical input to the transducer to produce a wave. The transducer, sometimes known as a pulser/receiver, is responsible for converting energy in the electrical form to mechanical and back again. Piezoelectric crystal is used in a transducer because it is capable of changing its dimensions from sending a signal to retrieving it; these types range in frequency of waves from 2 MHz to 10 MHz (Povey and McClements 1988). Important factors to consider when choosing a transducer are its diameter (depends on desired region of detection within material), frequency ranges (high or low intensity), and acoustic matching. Lastly, the electrical signal is reflected back and goes through the digitizer which converts it from an analog to digital signal. From this, the signal is then displayed on either an oscilloscope or computer screen and is then ready for further evaluation.

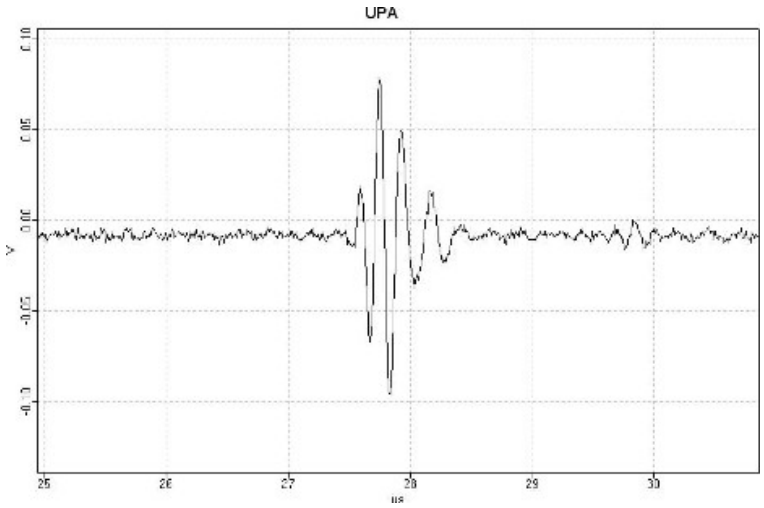

Figure 2.10. Ultrasound signal using a pulse-echo technique

There are different techniques by which the signal is sent but for this study the pulse-echo method will be addressed. As stated previously, the concept of reflectance is important for opaque, dense materials and therefore with on-line measurements it is vital to use a combination transducer/receiver and also a pulse-echo technique. The ultrasonic pulse, once converted from an electrical signal, goes through the sample, hits a solid wall on the other side, and is then reflected back to the transducer. The resulting signal is not one constant sinuidal wave but instead a series of echoes attributable to the portion of acoustic wave that was received back (McClements 1997). This signal gives information useful for determinating ultrasonic properties and furthermore, structural and physical characteristics of the material being tested.

References

Altomare, R.E., Ghossi, P., 1986. An analysis of residence time distribution patterns in a twin screw cooking extruder. Biotechnology Progress 2, 157-163.

Apruzzese, F., Balke, S.T., Diosady, L.L., 2000. In-line colour and composition monitoring in the extrusion cooking process. Food Research International 33, 621-628.

Balasubramanian, S., Singh, N., 2007. Effect of extrusion process variables and legumes on corn extrudates behaviour. Journal of Food Science and Technology-Mysore 44, 330-333.

BeMiller, J.N., Whistler, R.L., 1996. Food Chemistry, 3rd ed. Taylor & Francis Group, LLC, Boca Raton.

Bookwalter, G.N., Lyle, S.A., Nelsen, T.C., 1991. Enzyme inactivation improves stability of self-rising corn meals. Journal of Food Science 56, 494-496.

Camire, M.E., 1991. Protein functionality modification by extrusion cooking. Journal of the American Oil Chemists Society 68, 200-205.

Chung, O.K., 1991. Cereal Lipids. In K.J. Lorenz, K. Kulp (Eds.), Handbook of Cereal Science and Technology. Marcel Dekker, Inc., New York, pp. 497-553.

Collado, L.S., Corke, H., 2003. Characterization of Cereals and Flour. Marcel Dekker, Inc., New York.

Colonna, P., Mercier, C., 1983. Macromolecular modifications of manioc starch components by extrusion cooking with and without lipids. Carbohydrate Polymers 3.

Colonna, P., Tayeb, J., Mercier, C., 1989. Extrusion Cooking of Starch and Starchy Products. In C. Mercier, P. Linko, J.M. Harper (Eds.), Extrusion Cooking. American Association of Cereal Chemists, Inc., St. Paul, pp. 247-319.

Della Valle, G., Quillien, L., Gueguen, J., 1994. Relationships between processing conditions and starch and protein modifications during extrusion-cooking of pea flour. Journal of the Science of Food and Agriculture 64, 509-517.

Ding, Q.-B., Ainsworth, P., Plunkett, A., Tucker, G., Marson, H., 2006. The effect of extrusion conditions on the functional and physical properties of wheat-based expanded snacks. Journal of Food Engineering 73, 142-148.

Evers, A.D., Blakeney, A.B., L, O., Brien, 1999. Cereal structure and composition. Australian Journal of Agricultural Research 50.

Faubion, J.M., Hoseney, R.C., 1982. High-temperature short-time extrusion cooking of wheat-starch and flour .1. Effect of moisture and flour type on extrudate properties. Cereal Chemistry 59, 529-533.

Ferraro, J.R., Nakamoto, K., 1994. Introductory Raman Spectroscopy. Academic Press, Inc., San Diego.

Fletcher, S.I., Richmond, P., Smith, A.C., 1985. An experimental study of twin-screw extrusion cooking of maize grits. Journal of Food Engineering 4.

Freeman, S.K., 1974. Applications of Laser Raman Spectroscopy. John Wiley & Sons, Inc. , New York.

Friedman, M., 1996. Nutritional value of proteins from different food sources. A review. Journal of Agricultural and Food Chemistry 44, 6-29.

Guha, M., Ali, S.Z., Bhattacharya, S., 1997. Twin-screw extrusion of rice flour without a die: Effect of barrel temperature and screw speed on extrusion and extrudate characteristics. Journal of Food Engineering 32.

Hager, D.F., 1984. Effect of extrusion upon soy concentrate solubility. Journal of Agricultural and Food Chemistry 32, 293-296.

Harmann, D.V., Harper, J.M., 1973. Effect of extruder geometry on torque and flow. American Society of Agricultural Engineering 16, 1175-1178.

Harper, J.M., 1989. Food Extruders and Their Applications. In C. Mercier, P. Linko, J.M. Harper (Eds.), Extrusion Cooking. American Association of Cereal Chemists, Inc., St. Paul, pp. 1-15.

Hermansson, A.M., Svegmark, K., 1996. Developments in the understanding of starch functionality. Trends in Food Science & Technology 7, 345-353.

Howe, A.M., Mackie, A.R., Robins, M., 1986. Technique to measure emulsion creaming by velocity of ultrasound. Journal of Dispersion Science and Technology 7, 13.

Ikeda, S., Li-Chan, E.C.Y., 2004. Raman spectroscopy of heat-induced fine-stranded and particulate β-lactoglobulin gels. Food Hyrdocolloids 18, 9.

Jeunink, J., Cheftel, J.C., 1979. Chemical and physciochemical changes in field bean and soy proteins texturized by extrusion. Journal of Food Science 44, 5.

Johnson, L.A., 1991. Corn: Production, Processing, and Utilization. In K.J. Lorenz, K. Kulp (Eds.), Handbook of Cereal Science and Technology. Marcel Dekker, Inc., New York, pp. 55-132.

Jowitt, R., 1974. The terminology of food texture. In, Journal of Texture Studies. pp. 351-358.

Kent, N.L., Evers, A.D., 1994. Technology of Cereals, 4th ed. CRC Press, Cambridge.

Kizil, R., Irudayaraj, J., Seetharaman, K., 2002. Characterization of irradiated starches by using FT-Raman and FTIR spectroscopy. Journal of Agricultural and Food Chemistry 50, 3912-3918.

Li-Chan, E.C.Y., 1996. The applications of Raman spectroscopy in food science. Trends in Food Science & Technology 7, 361-370.

Liu, Y., Hsieh, F., Heymann, H., Huff, H.E., 2000. Effect of process conditions on the physical and sensory properties of extruded oat-corn puff. Journal of Food Science 65, 1253-1259.

Ma, C.-Y., Phillips, D.L., 2002. FT-Raman Spectroscopy and Its Applications in Cereal Science. Cereal Chemistry 79, 171-177.

Maga, J.A., 1991. Cereal-Based Snack Foods. In K.J. Lorenz, K. Kulp (Eds.), Handbook of Cereal Science and Technology. Marcel Dekker, Inc., New York, pp. 793-814.

Maga, J.A., 2000. Handbook of Cereal Science and Technology. In K.J. Lorenz, K. Kulp (Eds.), Cereal-based Snack foods. CRC Press, Manhattan.

Martelli, F., 1967. Single- and twin-screw extruders - a technical comparison. Spe Journal 23, 53.

McClements, D.J., 1995. Advances in application of ultrasound in food analysis and processing. Trends in Food Science & Technology 6, 7.

McClements, D.J., 1997. Ultrasonic characterization of foods and drinks: Principles, methods, and applications. Critical Reviews in Food Science and Nutrition 37, 1-46.

Pelletier, M.J., 1999. Analytical Applications of Raman Spectroscopy. Blackwell Science Ltd. , Ann Arbor.

Povey, M.J.W., Harden, C.A., 1981. An application of the ultrasonic pulse echo technique to the measurement of crispness of biscuits. Journal of Food Technology 16, 9.

Povey, M.J.W., McClements, D.J., 1988. Ultrasonics in food engineering. Part I: Introduction and experimental methods. Journal of Food Engineering 8, 217-245.

Ranhotra, G.S., 1991. Nutritional Quality of Cereals and Cereal-Based Foods. In K.J. Lorenz, K. Kulp (Eds.), Handbook of Cereal Science and Technology. Marcel Dekker, Inc., New York, pp. 845-861.

Rose, D.J., Ogden, L.V., Dunn, M.L., Pike, O.A., 2008. Enhanced lipid stability in whole wheat flour by lipase inactivation and antioxidant retention. Cereal Chemistry 85, 218-223.

Salazar, J., TurÛ, A., Ch·vez, J.A., GarcÌa, M.J., 2004. Ultrasonic inspection of batters for on-line process monitoring. Ultrasonics 42, 155-159.

Senanayake, S., Clarke, B., 1999. A simplified twin screw co-rotating food extruder: design, fabrication and testing. Journal of Food Engineering 40, 129-137.

Sharp, R.N., 1991. Rice: Production, Processing, and Utilization. In K.J. Lorenz, K. Kulp (Eds.), Handbook of Cereal Science and Technology. Marcel Dekker, Inc., New York, pp. 301-329.

Singh, B., Sekhon, K.S., Singh, N., 2007. Effects of moisture, temperature and level of pea grits on extrusion behaviour and product characteristics of rice. Food Chemistry 100.

Smith, E., Dent, G., 2005. Modern Raman Spectroscopy - A Practical Approach. John Wiley & Sons, Ltd, West Sussex, England.

Stanley, D.W., 1989. Protein Reactions During Extrusion Processing. In C. Mercier, P. Linko, J.M. Harper (Eds.), Extrusion Cooking. American Association of Cereal Chemists, Inc., St. Paul, pp. 321-341.

Stevenson, C.L., Vo-Dinh, T., 1996. Modern Techniques in Raman Spectroscopy. John Wiley & Sons Ltd., West Sussex.

Stojceska, V., Ainsworth, P., Plunkett, A., Ibanoglu, S., 2009. The effect of extrusion cooking using different water feed rates on the quality of ready-to-eat snacks made from food by-products. Food Chemistry 114, 226-232.

van der Veen, M.E., van Iersel, D.G., van der Goot, A.J., Boom, R.M., 2004. Shear-induced inactivation of alpha-amylase in a plain shear field. Biotechnology Progress 20, 1140-1145.

Vessa, J.A., 1990. Processing characteristics of kneading single-screw vs corotating twin-screw cereal extrusion. Cereal Foods World 35, 1162.

Zheng, X.G., Wang, S.S., 1994. Shear-induced starch conversion during extrusion. Journal of Food Science 59, 1137-1143.

CHAPTER 3

EFFECT OF EXTRUSION CONDITIONS ON THE FINAL PROPERTIES OF AN EXPANDED CEREAL SNACK[1]

[1] Miller, L.R., and J.H. Mulligan. To be submitted to *Journal of Cereal Science*

Abstract

Processing cereal-based snacks by extrusion cooking has become a common practice due to the overwhelming advantages it possesses over traditional methods. To increase its efficiency, an understanding of each independent variable's (screw speed, barrel temperature, and feed moisture) influence on the final product's characteristics is essential. In this study, three formulations of a cereal snack were extruded at a temperature of 90°C throughout the barrel; a constant screw speed of 220, 280, or 340 RPM was used for separate runs. One formulation was extruded at 280 RPM with varying degrees of temperature: 90, 100, 110, 120°C throughout the barrel, and 90, 100, 110°C progressively down the barrel. A 3-point bend analysis was performed on the extrudate as well as MicroCT evaluations and Minolta colorimeter readings. The results show that temperature, formulation, and screw speed have a significant effect on texture variables and only temperature is significantly associated with color values.

1. Introduction

Extrusion cooking has become an increasingly popular technique for the manufacture of cereal-based snacks largely due to its high efficiency. This method of processing encompasses cooking, kneading, forming, and shaping and most often with a co-rotating twin-screw configuration when cereals are a part of the formulation. Twin-screw extruders provide a greater level of shear and ingredient distribution in the dough and are also able to utilize the several processing parameters to a better degree. Independent variables associated with extrusion are product formulation, residence time, barrel temperature, screw speed, feed rate, die profile, and screw configuration; to control the product quality a good understanding of their effects is

important (Ding et al. 2006). Properties of an extrudate often altered by extrusion conditions are expansion, color, and overall textural characteristics (Harmann and Harper 1973).

Expansion is determined by the structure of the final product which, in turn, is linked with the texture. It is affected by the initial snack formulation because the greater amount of starch present the higher the expansion yet also if the starch undergoes a high degree of gelatinization, the expansion will also increase. The opposite case lies for protein incorporation into a product as well as fiber. Feed moisture has been found to have a negative effect on product expansion mostly due to the change in both pressure and viscosity throughout the barrel (Singh et al. 2007). Increasing the feed moisture when all other variables remain constant has shown to decrease the degree of starch conversion which creates a lower viscous dough with a lower pressure difference from the atmosphere yielding a lower expansion (Kokini et al. 1992). Temperature is directly related to the increase in expansion and is therefore the most common parameters altered to establish a specific product quality followed by screw speed. Temperature increase allows for a phase transition of the water incorporated into the dough to occur and results in a higher amount of flashing off when it exits the die (Fletcher et al. 1985).

Color values L^*, a^*, and b^* have previously been reported as a significant factor of product temperature during extrusion. Temperature has been shown to have a large impact on the definitive color often associated with its impact on expansion. Feed moisture also has a significant effect on color values whereas screw speed has not (Lei et al. 2007).

Understanding the extent to which extrusion independent variables can alter the overall textural characteristics is essential to optimizing consumer acceptability. Specific texture descriptors, hardness, crispness, and brittleness, are best used when identifying traits of a cereal-based product. Hardness (N) is established by the maximum peak force require to break the

product. Brittleness is associated with the distance necessary to fracture the extrudate with crispness being a function of brittleness while also incorporating a detectable sound when broken (Jowitt 1974). These variables were examined by Altan and others (2008) who determined that screw speed had no overall effect on the textural properties of a barley flour extrudate whereas product temperature had a very significant effect on all factors.

As extrusion technology continues to grow, it is vital to establish a known effect capable of determining the optimal conditions necessary for various types of products. The purpose of this study was to determine the effect of independent extrusion variables on the textural characteristics as well as the color and expansion of a cereal-based snack with varying amounts of protein and starch. It was performed with three screw speeds (220, 280, 340 RPM), three formulations with increasing ratios of protein to starch, and varying temperatures throughout the barrel, from 90°C to 120°C.

2. Materials and Methods

2.1 *Materials*

Chickpea flour was obtained from Garden Valley Corporation (Sutherlin, OR). Corn flour was supplied by Bunge North America (St. Louis, MO). Oat flour was obtained from Grain Millers, Inc. (St. Ansgar, IA). Advanced Food Systems, Inc. (Somerset, NJ) supplied the corn starch, Actobind DC 900. Tomato powder was obtained from Valley Sun (Newman, CA). Ground raw hazelnuts were provided by the Hazelnut Growers of Oregon (Cornelius, OR) and stored at 2.7°C. All other ingredients were stored at room temperature.

2.2 *Preparation of Cereal Snack*

Table 3.1 displays the ingredient distribution for each formulation on a 3.632 kg basis. The ingredients were weighed out then placed into a large Kramer Grebe bowl chopper (CFS, Wallau, Germany) and mixed for 10 minutes. The mixtures were stored in large white plastic bags until use. Nine batches of each formulation were produced.

2.3 *Extrusion Processing*

A MPF30 laboratory-scale co-rotating twin-screw extruder (APV Baker, Ltd., Grand Rapids, MI) was used throughout this experiment. The barrel length to diameter (L/D) ratio was 25:1 with a screw diameter of 30 mm and a length of 750 mm. The extruder contained five temperature zones controlled by electric heat and circulating cooling water. The design was a clamshell barrel with a 4 mm circular die at the end. The screw configuration is shown in Figure 3.1 and included (on each screw) three 1.5D feed screws, one 1D screw, five forward feeding kneading blocks, three 1.5D feed screws, 9 reverse feed kneading blocks, one 1D screw, two 1.5D screws, one 1D screw, 10 forward feed kneading blocks, two 1D screws, four kneading blocks feeding forward, and a tight helix screw to increase forward movement.

The screw speed was controlled by a computer system that also displayed the barrel temperature zones, torque, pressure at die, and cooling system. The cereal snack mixture was conveyed into the extruder by a K2 volumetric feeder (K-Tron, Pitman, NJ) at different rates in conjunction with deionized water introduced via a Bran+Leubbe® metering pump (Buffalo Grova, IL) to reach a moisture content of 16% as shown in Table 3.2. After exiting the die, the extrudates were then cut by hand at 40 cm and dried in an Alkar smoker (Lodi, WI) at 100°C

until reaching a final moisture content of 2-4%. Samples were then packaged in heat sealed Cryovac bags and held at room temperature in dark conditions.

2.4 *Moisture Analysis*

The moisture content of the dried product was determined using a Mettler-Toledo Moisture Analyzer (Greifensee, Switzerland) in triplicate.

2.5 *Expansion Ratio*

The expansion ratio (or sectional expansion) was determined using Vernier calipers to measure the diameter (mm). This value was then used in the ratio of the diameter of the extrudate over the diameter of the die. (Alvarez-Martinez et al. 1988) Five replicates were performed on each batch.

2.6 *Texture Analysis*

A 3-point bend test was performed on a TA-XT2 (Texture Technologies, Scarsdale, NY) to obtain information on the hardness, brittleness, and crispness of the cereal snack. Hardness was reported as the maximum require force (N) to break the extrudate. Brittleness was measured as the distance (mm) on the force-distance curve where the sample broke where crispness utilized the slope of the line (N/mm). All samples were cut before testing by a Hitachi CB6Y bandsaw (Hitachi Koki, Ltd., Atlanta, GA) to 7 cm in length and those with equal diameters were used. The following settings were applied: 5 kg load cell, measure force in compression, return to start, 40 mm return distance, pretest speed of 1 mm/sec, test speed of 3 mm/sec, post-test

speed of 10 mm/sec, 5 mm distance, trigger force of 50 kg. This analysis was completed on five replicates per batch.

2.7 *Color Analysis*

The color of the samples was evaluated using a CR-400/410 Minolta colorimeter (Osaka, Japan) after first being calibrated to display accurate L^*, a^*, and b^* values. For each batch the samples were stacked into rows five deep and across on white paper to discourage inaccurate light reflectance. A test was performed in three different locations in order to take a representative sample of the material. From the a^* and b^* values hue angle and chroma were calculated using the following equations: hue angle = $\arctan (b^*/a^*)$, chroma = $(a^{*2}+ b^{*2})^{1/2}$.

2.8 *MicroCT Evaluation*

A Skyscan1072 MicroCT instrument (MicroPhotonics, Inc., Allentown, PA) was utilized to create a visual on the air distribution throughout each sample. Samples were 3 cm in length and stabilized within the chamber by the use of clay. An x-ray source at 54 km/185 uA rotated 180° with each step being 0.68° and an exposure of 6.8 seconds. The gain was 1.0 and an aluminum filter of 1 mm in width was in place to clarify the image. During both acquiring the image and reconstruction, several parameters changed for each sample as displayed in Table 3.3.

2.9 *Data Analysis*

Statistical Analysis Software (Version 9.1e, SAS Institute Inc., Cary, NC) was used to compute ANOVA with significance established at $P < 0.05$ by generalized linear modeling. Also established was Pearson correlation coefficient and linear regression.

3. Results and Discussion

3.1 *Expansion Ratio*

The expansion ratio was determined by the diameter of the extrudate once drying had occurred and also from images produced by a MicroCT Skyscan. Table 3.4 shows that depending on the protein to starch ratio within the formulation the product does not expand differently. Similarily, the screw speed from one extrusion run to another did not have a significant effect on the expansion ratio (Table 3.6). The lack of effect from screw speed could be attributable to the decrease in barrel fill as a result of decreased residence time. As temperature increases, it superheats the water and allows the phase transition to occur more readily which yields more air production within the extrudate (Figure 3.2). As the temperature rises from 90°C to 90, 100, 110°C the expansion ratio increases from 1.50 to 3.17 ($P < 0.05$). The increase in expansion as temperature rises is shown in Table 3.8.

3.2 *Color values*

The change in color during extrusion can be an indicator of the degree of thermal and shear treatment along the barrel (Chen et al. 1991). Color values used often in deciphering color are L^*, a^*, and b^*, which signify the lightness/darkness, redness, and yellowness, respectively. The color values for varying degrees of screw speeds and temperature within each formulation are shown in Tables 3.7 and 3.9. Change in formulations from low to high protein to starch ratios had a significant effect on L^* ($P < 0.05$), a^* ($P < 0.05$), and b^* ($P < 0.05$) (Table 3.5). L^* values between Formulations A and B remained similar whereas the value for formulation C drastically increased signifying the lightness that occurs. The reported a^* and b^* values were significantly different in Formulation C as compared to A and B. Hue angle rose significantly in response to

the increase in protein, getting closer to 90° but in the orange range. The color intensity of a material is identified by the chroma and, in the case of formulation changes, remained close between Formulations A and B but significantly differed from Formulation C ($P < 0.05$). In conjunction with what was reported by Altan and others (2008), screw speed did not have a significant influence on L^*, a^*, and b^* ($P > 0.05$) as shown in Table 3.7 or hue angle and chroma data. Increased screw speed results in a decreased residence time which leads to a shorter exposure to heat thus the color has less change.

Temperature had the greatest overall effect on L^* compared to other parameters; there was a significant increase, from 37.48 to 53.24 (Table 3.9), exemplifying its significance ($P < 0.05$). This corresponds to the data published by Ilo and others (1999) during the extrusion of maize grits. The values for hue angle grew from 61.28 to 75.07, in the orange range, while chroma also increased, enhancing the purity of the color; these factors were both significantly affected by the change in temperature. A combined effect between temperature and the heightened expansion would also create a lighter extrudate as shown.

3.3 *Textural characteristics*

The effect of formulation on the hardness of the extrudate was found to be significant ($P < 0.05$) as displayed in Table 3.10. As the formulation's protein to starch ratio rose, the hardness values for Formulation C greatly decreased as did those affected by screw speed ($P < 0.05$). For Formulations A and B, the hardness values were greatest at screw speeds of 280 RPM. The change in hardness due to temperature was shown to be significant ($P < 0.05$) on the extrudate with 90°C and 100°C being significantly different than the rest. Table 3.8 shows that as temperature increased, the hardness of the extrudate dropped from 48.07 N to 7.77 N, a visible

indicator of its ability to alter textural properties which correlates well with the findings of Ding and others (2006). The high temperatures in the extruder allow for the phase transition of water within the dough and flashing off as steam once it is subjected to atmospheric pressure. This high degree of air incorporation throughout the extrudate creates a product that is more easily fractured requiring less force.

The distance necessary to puncture the product determines the brittleness and was found to be dependent on several factors. Formulations and screw speed showed significance in altering brittleness (mm) ($P > 0.05$). Formulation C tended to be the most brittle overall meaning it required less distance to fracture; the brittleness values ranged from 0.202 to 1.018 mm between formulations. As temperature increased there was a significant decrease in brittleness ($P < 0.05$) also attributable to the larger expansion; 90°C and 100°C were again significantly different from the other temperatures used during extrusion.

The crispness is associated with the slope of the line and was shown to relate significantly to the formulation of the product when comparing Formulations A and B to C ($P < 0.05$). Crispness depicts a product that is brittle yet also obtains a specific sound when broken. The values for crispness had a very large range from Formulation C to Formulations A and B, 5.25 to 27.29 mm^{-1}; crispness was lowest in the low starch formulation C. The change in screw speeds between batches produced significant differences in the crispness of the product and as with the other textural properties, there was a significant indirect relationship with temperature ($P < 0.05$). Overall, the combination of screw speed and formulation can be used to predict textural outcomes since the correlation was high with all factors: hardness ($R^2 = 0.906$), brittleness ($R^2 = 0.841$), and crispness ($R^2 = 0.787$).

3.4 *Correlation between extrudate properties*

Table 3.11 identifies the relationship between extrudate properties and found the greatest correlation between hardness and brittleness ($P < 0.05$); there is a direct relationship between these properties. All of the texture properties had a negative yet significant ($P < 0.05$) correlation with both L^* and b^* resulting in a lighter and more yellow product as they decrease. The significant correlation ($P < 0.05$) with a^* supports the visual understanding that the redness of the extrudate increases along with hardness, brittleness, and crispness. As shown in Table 3.11, as the extrudate becomes lighter the a^* value significantly decreases ($P < 0.05$) and b^* significantly increases ($P < 0.05$). There is no significant relationship between color values independent of L^*.

4. **Conclusion**

Independent extrusion variables produce significant changes within cereal-based snacks. Temperature had the greatest affect on texture and color, and the only significant effect on expansion properties due to the heightened air incorporation once the product exited the die; production formulation and screw speed also produced significant differences in the extrudate's physical properties and can be adjusted according to the desired outcome. The negative correlation between textural variables and L^* and b^* indicate that the product will become lighter as the amount of force and distance required to fracture the extrudate decreases.

References

Altan, A., McCarthy, K.L., Maskan, M., 2008. Extrusion cooking of barley flour and process parameter optimization by using response surface methodology. Journal of the Science of Food and Agriculture 88, 1648-1659.

Alvarez-Martinez, L., Kondury, K.P., Harper, J.M., 1988. A general-model for expansion of extruded products. Journal of Food Science 53, 609-615.

Chen, J., Serafin, F.L., Pandya, R.N., Daun, H., 1991. Effect of extrusion conditions on sensory properties of corn meal extrudates. Journal of Food Science 56, 6.

Ding, Q.-B., Ainsworth, P., Plunkett, A., Tucker, G., Marson, H., 2006. The effect of extrusion conditions on the functional and physical properties of wheat-based expanded snacks. Journal of Food Engineering 73, 142-148.

Fletcher, S.I., Richmond, P., Smith, A.C., 1985. An experimental study of twin-screw extrusion cooking of maize grits. Journal of Food Engineering 4.

Harmann, D.V., Harper, J.M., 1973. Effect of extruder geometry on torque and flow. American Society of Agricultural Engineering 16, 1175-1178.

Ilo, S., Berghofe, E., 1999. Kinetics of colour changes during extrusion cooking of maize grits. Journal of Food Engineering 39, 8.

Jowitt, R., 1974. The terminology of food texture. In, Journal of Texture Studies. pp. 351-358.

Kokini, J.L., Change, C.N., Lai, L.S., 1992. The role of rheological properties on extrudate expansion. In J.L. Kokini, C.T. Ho, M.V. Karwe (Eds.), Food Extrusion Science and Technology. Marcel Dekker, New York, pp. 631-652.

Lei, H.W., Fulcher, R.G., Ruan, R., van Lengerich, B., 2007. Assessment of color development due to twin-screw extrusion of rice-ghtcose-lysine blend using image analysis. Lwt-Food

Science and Technology 40, 1224-1231.

Ozer, E.A., Ibanoglu, S., Ainsworth, P., Yagmur, C., 2004. Expansion characteristics of a nutritious extruded snack food using response surface methodology. European Food Research Technology 218, 6.

Singh, B., Sekhon, K.S., Singh, N., 2007. Effects of moisture, temperature and level of pea grits on extrusion behaviour and product characteristics of rice. Food Chemistry 100.

Table 3.1. Ingredient formulations used during the extrusion of a cereal snack on a 3.632 kg basis (Ozer et al. 2004)

Formulation	Chickpea Flour (kg)	Corn Flour (kg)	Oat Flour (kg)	Cornstarch (kg)	Tomato Powder (kg)	Ground Raw Hazelnuts (kg)
A	1.0896	.7264	.7264	.5448	.3632	.1816
B	1.2712	.7264	.7264	.3632	.3632	.1816
C	1.4528	.7264	.7264	.1816	.3632	.1816

Table 3.2. Independent extrusion parameters utilized to control processing

Formulation	Batch	Feeder Speed (RPM)	Barrel Temp* (°C)	Screw Speed (RPM)	Drying Time (hrs)
A	1	300	90	220	8
	2	300	90	280	8
	3	300	90	340	8
	4	300	90	280	5
	5	300	100	280	5
	6	300	110	280	5.5
	7	300	120	280	5
	8	300	90, 100, 110	280	5
B	1	295	90	220	9
	2	295	90	280	9
	3	295	90	340	9
C	1	300	90	220	5
	2	300	90	280	5
	3	300	90	340	5

*Actual temperatures were ±2°C

Table 3.3 MicroCT values for both image capture and configuration

Sample	Y-Position	Magnification	Compensation
A_1	- 5	29	- 5.5
A_2	- 5	30	- 5.5
A_3	- 5	32	- 5.0
A_4	- 5	29	- 4.5
A_5	- 5	22	- 5.0
A_6	- 6	22	- 4.5
A_7	- 4	18	- 2.5
A_8	- 5	21	- 4.0
B_1	- 5	29	- 6.0
B_2	- 4	30	- 5.0
B_3	- 5	29	- 5.0
C_1	- 4	27	- 5.0
C_2	- 5	26	- 4.5
C_3	- 5	26	- 5.0

Table 3.4. Mean data of textural responses to formulation changes

Formulation	Hardness (N)	Brittleness (mm)	Crispness (mm^{-1})	Expansion ratio
A	29.23^{a}	1.02^{a}	27.29^{a}	1.53^{a}
B	29.94^{a}	0.75^{b}	25.77^{a}	1.50^{a}
C	1.16^{b}	0.20^{c}	5.25^{b}	1.42^{a}

Means with the same letter in each column are not significantly different ($P > 0.05$)

Table 3.5. Mean data of color responses to formulation changes

Formulation	L*	a*	b*	Hue angle	Chroma
A	44.91[b]	7.92[a]	20.99[b]	68.96[b]	22.52[b]
B	44.44[b]	7.55[a]	19.38[b]	68.47[b]	20.87[b]
C	54.26[a]	5.31[b]	24.19[a]	77.62[a]	24.77[a]

Means with the same letter in each column are not significantly different ($P > 0.05$)

Table 3.6. Mean data of textural responses to screw speed changes

Speed (RPM)	Hardness (N)	Brittleness (mm)	Crispness (mm^{-1})	Expansion ratio
220	15.84^{a}	0.58^{b}	19.27^{ab}	1.50^{a}
280	24.84^{a}	0.80^{a}	22.87^{a}	1.47^{a}
340	16.88^{a}	0.53^{b}	16.18^{b}	1.47^{a}

Means with the same letter in each column are not significantly different ($P > 0.05$)

Table 3.7. Mean data of color responses to screw speed changes

Speed (RPM)	**L***	**a***	**b***	**Hue angle**	**Chroma**
220	49.98[a]	6.29[a]	22.08[a]	73.85[a]	22.99[a]
280	46.59[a]	7.24[a]	21.31[a]	70.17[a]	22.20[a]
340	46.12[a]	7.51[a]	20.86[a]	70.08[a]	22.74[a]

Means with the same letter in each column are not significantly different ($P > 0.05$)

Table 3.8. Mean data of texture responses to temperature changes

Temperature (°C)	**Hardness (N)**	**Brittleness (mm)**	**Crispness (mm^{-1})**	**Expansion ratio**
90	48.07[a]	1.32[a]	37.65[a]	1.50[c]
100	49.14[a]	1.39[a]	36.66[ab]	1.92[c]
110	23.30[b]	0.66[b]	30.71[b]	2.42[b]
120	8.77[c]	0.50[b]	18.43[c]	2.75[ab]
90,100, 110	7.77[c]	0.39[b]	17.81[c]	3.17[ab]

Means with the same letter in each column are not significantly different ($P > 0.05$)

Table 3.9. Mean data of color responses to temperature changes

Temperature (°C)	L*	a*	b*	Hue angle	Chroma
90	37.84[b]	8.53[a]	15.57[b]	61.28[b]	17.76[b]
100	36.87[b]	6.19[b]	11.75[c]	61.16[b]	13.32[c]
110	51.07[a]	5.62[b]	18.12[ab]	73.34[a]	18.91[ab]
120	53.24[a]	5.35[b]	20.54[a]	74.65[a]	19.01[ab]
90,100, 110	52.11[a]	4.89[b]	18.37[ab]	75.08[a]	21.29[a]

Means with the same letter in each column are not significantly different ($P > 0.05$)

Table 3.10. ANOVA of extrudate responses

Parameter	**Hardness (N)**	**Brittleness (mm)**	**Crispness (mm^{-1})**	**Expansion ratio**	**L^***	**a^***	**b^***
Formulation	**	**	**	NS	**	**	**
Screw Speed	**	**	**	NS	NS	NS	NS
Temperature	**	**	**	**	**	**	**

** indicates significance at P-value < 0.05

Table 3.11. Correlation coefficients between extrudate properties

	Hardness	Brittleness	Crispness	L^*	a^*	b^*
Hardness	1	0.9527*	0.9041 n.s.	- 0.9431*	0.7081*	- 0.7845*
Brittleness		1	0.8184 n.s.	- 0.8156*	0.6143*	- 0.6924*
Crispness			1	- 0.6772*	0.4540*	- 0.7039*
L^*				1	- 0.7985*	0.7563*
a^*					1	- 0.2962 n.s.
b^*						1

(*) Significant at $P < 0.05$; n.s., not significant

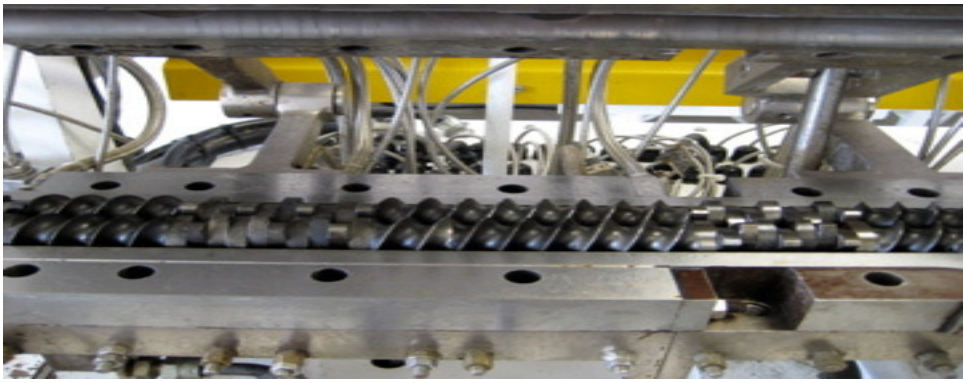

Figure 3.1. Twin-screw, co-rotating, intermeshing extruder configuration

a. b.

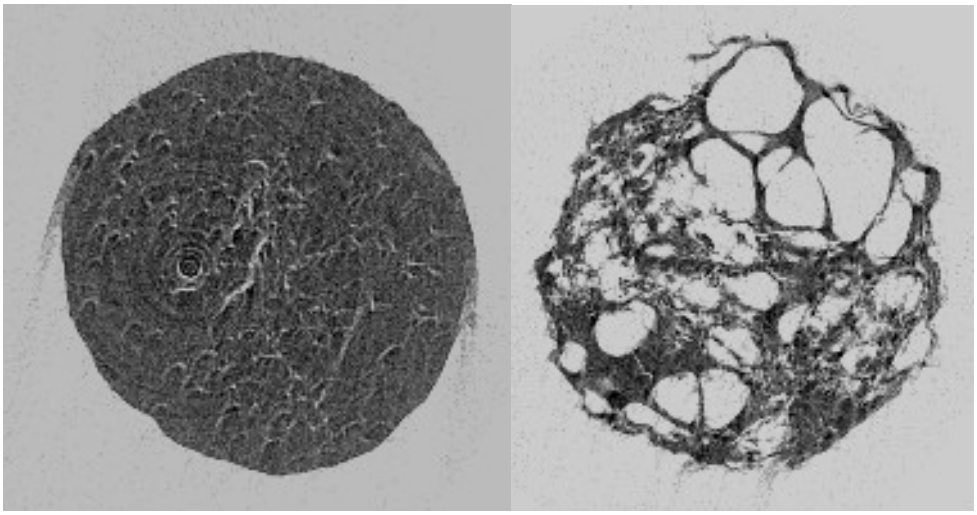

Figure 3.2 Cross-section of extrudate at (a) 90°C and (b) 120°C

CHAPTER 4

ON-LINE MONITORING AND PROCESS-PROPERTY-STRUCTURE RELATIONSHIPS IN EXTRUDED CEREAL PRODUCTS[1]

[1] Miller, L. M. and J. H. Mulligan. To be submitted to *Journal of Food Chemistry*

Abstract

On-line monitoring devices used during extrusion are fast and precise tools that enable characterization of materials during processing. Raman spectroscopy and non-destructive ultrasound techniques were utilized on-line during extrusion cooking of a cereal snack in this study. The objectives were to determine the chemical bonds present during extrusion and to establish a relationship between on-line monitoring and final textural properties of a cereal product. Three product formulations were extruded at screw speeds 220, 280, and 340 RPM with varying temperatures; on-line measurements were taken at several locations. After drying, a 3-point bend test analyzed the hardness, crispness, and brittleness of the product. Common Raman bands in increased protein to starch ratio formulations, 1125 cm^{-1}, 1290 cm^{-1}, and 1470 cm^{-1}, were able to withstand high amounts of shear yet were broken at temperatures above 90°C. The results showed that attenuation is a good predictor for both hardness and brittleness values ($P < 0.05$).

1. Introduction

Cereals are the most abundantly grown food worldwide and supply more energy in the diet than any other crop. They are largely made up of proteins, lipids, and carbohydrates within which is starch, which govern many of the functional properties (Evers et al. 1999). Starch is composed of amylose and amylopectin and as the steps of gelatinization take place during processing much of the amylose is leached out and replaced by water (Collado and Corke 2003). This endothermic process creates an amorphous state throughout the granule and can largely affect the gel strength and textural characteristics of a cereal product (Hermansson and Svegmark 1996). Previously, these starchy products have been produced in batch processes that require

extended periods of time, much space, and can withstand only limited formulation variability. In recent years, the utilization of extrusion cooking to adequately knead, form, cook, and shape cereal-based products has been on the rise (Mercier et al. 1989). Extrusion provides high levels of shear force and greater efficiency in one device yielding more consistent product quality.

One of the most useful tools regarding extrusion is the ability to control specific parameters that can alter the physicochemical properties of the final product. The solid feed rate, screw speed, (Altomare and Ghossi 1986) feed moisture, residence time, barrel temperature, (Martelli 1967) and die size are all factors that can be altered depending on the desired outcome. Dough characteristics change due to parameter adjustments and ingredient variability and can undergo numerous types of bond breaking or forming throughout the process. Primarily concerning starch-based snacks is the formation of cross-links, starch conversion, and protein denaturation; the ability to control these chemical transformations can directly attribute to textural properties within the extrudate (Colonna et al. 1989). To control parameters for product optimization on-line monitoring tools can be employed; they can provide decreased production time, cost, and overall waste while also obtaining a more thorough understanding of the true physicochemical characteristics of the material (Grenier and Bellon-Maurel 2003). On-line monitoring tools must be rapid, nondestructive, precise, and capable of working off of backscattering/reflectance in order to provide any benefit to the operator.

Raman spectroscopy is a tool that can achieve this while supplying information on the molecular structure of each component within the material being extruded yielding both qualitative and quantitative results. A laser beam of monochromatic light is imposed on a sample causing the photons to be both absorbed and reflected depending on the vibrational interactions. While a majority of the scattered light will have the same frequency as the incident beam, a small

fraction, about 1 in 10^7 photons, will have a change in energy and produce a different frequency of light (Smith and Dent 2005). This Raman scattering, while being a weak process, is proportional to the amount of analyte in a sample and is expressed as the wavenumber shift (Δcm^{-1}). Plotting the Raman intensity of light versus the wavenumber shift then produces a Raman spectrum used to establish bonding features.

While Raman spectroscopy provides extensive knowledge on the structural changes throughout extrusion, non-destructive ultrasound is necessary to comprehend the physical attributes of the material. It has been used for various applications, from detecting droplet sizes in emulsions (Howe et al. 1986) to determining the crispness of a biscuit (Povey and Harden 1981). Non-destructive ultrasound uses sound waves between frequencies of 2 to 10 MHz that do not alter the structural composition of the food. It is a precise method of evaluation that takes only 10 seconds on average to perform. The pulse-echo wave that is sent out is transmitted to the material and then reflects back providing an ultrasound signal of amplitude versus time. From this signal, characteristics of the wave such as the wavelength, attenuation, and velocity can be determined. These values are then used with mathematical theories to relate the ultrasonic properties to physical features of the product (McClements 1997).

Few studies have been done to create a better understanding of how on-line process monitoring can be utilized during the production of cereal-based products; this has resulted in the current study's design of using two on-line monitoring techniques, extrusion cooking, and textural measurements. The objectives of this study are to identify the peaks associated with cereal snack processing and to establish a relationship between on-line monitoring evaluations and the final textural properties of a cereal snack.

2. Materials and Methods

2.1 *Materials*

Chickpea flour was obtained from Garden Valley Corporation (Sutherlin, OR). Corn flour was supplied by Bunge North America (USA). Oat flour was obtained from Grain Millers, Inc. (St. Ansgar, IA). Advanced Food Systems, Inc. (Somerset, NJ) supplied the corn starch, Actobind DC 900. Tomato powder was obtained from Valley Sun (Newman, CA). Ground raw hazelnuts were provided by the Hazelnut Growers of Oregon (Cornelius, OR) and stored at 2.7°C. All other ingredients were stored at room temperature.

2.2 *Preparation of Cereal Snack*

Table 4.1 displays the ingredient distribution for each formulation on a 3.632 kg basis. The ingredients were weighed out then placed into a large Kramer Grebe bowl chopper (CFS, Wallau, Germany) and mixed for approximately 10 minutes. The mixtures were stored in large white plastic bags until use. Nine batches of each formulation were produced.

2.3 *Extrusion Processing*

A MPF30 laboratory-scale co-rotating twin-screw extruder (APV Baker, Ltd., Grand Rapids, MI) was used throughout this experiment. The barrel length to diameter (L/D) ratio was 25:1 with a screw diameter of 30 mm and a length of 750 mm. The extruder contained five temperature zones controlled by electric heat and circulating cooling water. The design was a clamshell barrel with a 4 mm circular die at the end. The screw configuration is shown by Figure 4.1 and included (on each screw) three 3D feed screws, one 1D screw, five forward feeding kneading blocks, three 1.5D feed screws, 9 reverse feed kneading blocks, one 1D screw, two

1.5D screws, one 1D screw, 10 forward feed kneading blocks, two 1D screws, four kneading blocks feeding forward, and a tight helix screw to increase forward movement.

The screw speed was controlled by a computer system that also displayed the barrel temperature zones, torque, pressure at die, and cooling system. The cereal snack mixture was conveyed into the extruder by a K2 volumetric feeder (K-Tron, Pitman, NJ) at different rates in conjunction with deionized water introduced via a Bran+Leubbe® metering pump (Buffalo Grova, IL) to reach a moisture content of 16% as shown in Table 4.2. The torque remained between 11-15% for each run. After exiting the die, the extrudates were then cut by hand at 40 cm and dried in an Alkar 1000 smoker (Lodi, WI) at 100°C until reaching a final moisture content of 2-4%. Samples were then packaged in heat sealed Cryovac bags and held at room temperature in dark conditions.

2.4 *Moisture Analysis*

The moisture content of the dried product was determined using a Mettler-Toledo Moisture Analyzer (Greifensee, Switzerland) in triplicate.

2.5 *Raman Evaluation*

For on-line monitoring a HRC-10HT Bruker Optics Sentinel Raman spectrometer (Bruker Optics, Billerica, MA) was used. A 785 nm diode laser with 500 mW of power was the excitation source. A background was collected for 20 seconds followed by the spectra for another 20 seconds in order to achieve an acceptable signal to noise (S/N) ratio; a charge-coupled device was also in place to decrease background noise. The spectral range was between 220 cm^{-1} and 2250 cm^{-1} with baseline correction and normalization taking place after collection

using Sure_Cal. The probe containing the laser was attached to a ring stand and placed above open ports along the extruder as shown in Figure 4.2. The distance of the ports from the beginning of the barrel were as follows: 43.49 cm, 68.26 cm, and 80.01 cm. A large, black plastic bag was draped over the Raman probe and extruder in order to create a dark environment throughout sampling. Raman spectra were taken in triplicate at each port for every sample.

2.6 *Ultrasound Analysis*

A UTEX UT-340 Process Analyzer (UTEX Scientific Instruments, Inc., Ontario, CA) coupled with a RF digitizer and probe was used for sending and receiving the ultrasonic signal at a frequency of 5 MHz. The scan duration was 10 seconds with a sampling interval of 0.25 seconds. The signal was displayed on a computer screen equipped with Inspectionware NDE Development Platform software; through this program the characteristics of the wave (velocity, wavelength, attenuation, frequency, amplitude) were evaluated. Five ultrasonic signals were acquired for each batch with the probe located at the end of the extruder barrel directly before the dough exited the die (Figure 4.2).

2.7 *Texture Analysis*

A 3-point bend test was performed on a TA-XT2 (Texture Technologies, Scarsdale, NY) to obtain information on the hardness, brittleness, and crispness of the cereal snack. Hardness was reported as the maximum required force (N) to break the extrudate. Brittleness was measured as the distance (mm) on the force-distance curve where the sample broke where crispness utilized the slope of the line (N/mm). All samples were cut before testing by a Hitachi CB6Y bandsaw (Hitachi Koki, Ltd., Atlanta, GA) to 7 cm in lengths and those with equal

diameters were selected for testing. The following settings were applied: 5 kg load cell, measure force in compression, return to start, 40 mm return distance, pretest speed of 1 mm/sec, test speed of 3 mm/sec, post-test speed of 10 mm/sec, 5 mm distance, trigger force of 50 kg. This analysis was completed on five replicates per batch.

2.8 *Data Analysis*

Statistical Analysis Software (Version 9.1e, SAS Institute Inc., Cary, NC) was used to compute ANOVA with significance established at $P < 0.05$ by generalized linear modeling. Also established was Pearson correlation coefficient and linear regression.

3. Results and Discussion

3.1 *Common Raman bands in cereal products*

Figure 4.3 shows the typical Raman spectrum of a cereal snack as analyzed during extrusion. Although water was added to the system in order to form the dough, it produces a very weak Raman scatter and therefore is not present within the spectra and does not alter the resulting evaluation. The first sharp peak present within the spectra of cereal-based products was a C-H stretch at 480 cm^{-1} due to the pyranose ring in the glucose unit (Tu et al. 1979); this is an indicator of polymerization in polysaccharides. The skeletal mode vibrations of this pyranose ring also produced bands at 560 cm^{-1}. In the region of 500-540 cm^{-1} there are several small peaks attributable to S-S stretching in the amino acid cystine. Disulfide bonds contribute significantly to the structural properties of proteins and are often seen before processing takes place. Additional small peaks occur at 670 and between 700-740 cm^{-1} all of which are vibrations from a C-S stretch in cysteine molecules. One of the largest peaks within the Raman spectra of cereal

snacks is at 840 cm^{-1}, and because of the ingredient variability, can be a function of either the phenol group of tyrosine or C-O bending in hydrocarbon chains (Li-Chan 1996).

A characteristic band of amylose appears at 1040 cm^{-1} as a result of C-O-H bending; this also contributes to the 1130 cm^{-1} peak which overlaps with the C-O vibration of hydrocarbon chains of lipids (Cael et al. 1973). The 1260-1290 cm^{-1} region of the Raman spectra is formed by both starch and protein molecules. Side chains of amylose, CH_2OH, coupled with either a N-H bend or C-N stretch of amide III create peaks of high intensity (Ellepola et al. 2006). This amide III is a good indicator of the secondary structure of protein as is amide I which shows up later in the spectra (Li-Chan 1996). The amino acid tryptophan displays a peak at 1360 cm^{-1} from the vibrations of the indole ring portion of the molecule. The presence of amino acids continues in the spectra at 1430 cm^{-1} attributable to the C=O stretch of COO^-. A CH_2 deformation occurs at 1460 cm^{-1} and CH_2 scissoring immediately after at 1500 cm^{-1} (Baeten et al. 1998). The indole ring of tryptophan produces another peak, yet a smaller one, at 1555 cm^{-1} (Nonaka et al. 1993). A peak at 1570 cm^{-1} is attributable to amide II. C=C stretching of lipids are present at 1640 cm^{-1} and 1655 cm^{-1}; a C=O stretch of amide I, a function of protein's secondary structure, also contributes to the 1655 cm^{-1} band (Ellepola et al. 2006). Lastly, at band at 1849 cm^{-1} is due to the presence of C-O stretching of hydrocarbon chains in lipids (Suetaka and Yates 1995).

3.2 *Change in Raman bands*

As different formulations, temperatures, and speeds were used during extrusion there was expected to be a change in the Raman bands. This can be in the form of shifts in wavenumber, decrease or increase in relative intensity, or the disappearance/appearance of bands due to processing and how it affects the dough. The Raman evaluation was taken at three different

locations progressively down the barrel (1, 2, and 3) with the extrusion parameters causing changes in each spectra. When observing the effect of speed there is an apparent change of bonding characteristics by the residence time. At the accelerated screw speed of 340 there will be a shorter residence time yielding greater shear levels but less cooking time. This enables bonds to stay intact as compared to screw speed of 220 that has a longer residence time and can often display increased bond breaking as a result. From the Raman spectra it was found that only at 280 RPM does a peak show up for C=C stretching at 1635 cm^{-1} in all locations. At speeds 280 and 340 RPM the 1125 cm^{-1} band for starch and lipid vibrations disappears from the spectra. The fastest screw speed of 340 RPM causes the appearance of amylose/amide III peak of 1290 cm^{-1} to be present in location 3, the port closest to the die.

Altering the formulation of the cereal snack greatly influenced the resulting Raman spectra. Only in formulation A did the 600 cm^{-1} band show up for the entire extruder length, an indicator of phenylalanine, whereas in this same formulation the 670-690 cm^{-1} band of cysteine was detectable solely in location 1. Formulations B and C had a commonality in that 1125 cm^{-1}, important for both starch and lipids, produced a peak at location 1, before any breakdown took place. In these formulations at locations 1 and 2 a 1470 cm^{-1} band attributable to CH_2 bending showed up, only in location 3 was the 1290 cm^{-1} peak apparent; this latter band is due to the amylose side chain and amide III vibrations. Formulation C incurred an amide II break at 1570 cm^{-1} in location 2 and then a disappearance of the 1525 cm^{-1} band for lipids in location 3.

The increase in temperature during extrusion produced not only visual but also many structural changes within the snack. It was only when the temperature was increased above 90°C did the C-O-H bending of starch and the C-O vibration of hydrocarbons chains band at 1125 cm^{-1} disappear from the spectra as shown by Figure 4.4. At location 1 at these high temperatures,

1630 cm^{-1} for lipids did not show and the intensity of the amylose band at 1039 cm^{-1} decreased as well as in location 2. Location 2 also produced a slight decrease in intensity of the 1849 cm^{-1} band due to C-O stretching. Two bands essential to the identification of proteins, 1297 cm^{-1} and 1327 cm^{-1} were not a part of the spectra in location 3; the breakdown of protein at escalated temperatures and shear levels is responsible for this lack of bonding.

3.3 *Correlation between Raman peak ratios and extrusion*

In an effort to establish a relationship between peak ratios acquired from the Raman spectra and specific parameters used during extrusion Pearson correlation coefficients were run. Peak ratios were first determined by using the relative Raman intensity of a peak over the relative Raman intensity of the peak at 840 cm^{-1}. This peak was used in the ratio because it was consistent in all spectra acquired during the study. Overall with speed, the correlation of peak ratios and extrusion variables was very low ($R^2 = 0.01$) and with no significance ($P > 0.05$). When broken down into location (1, 2, and 3) the test showed that there is also a low correlation ($R^2 = 0.029$) with location 1 with no significance ($P > 0.05$). At locations 2 and 3 there were negative correlations, $R^2 = -0.025$ and -0.007, respectively also with no significance. The speed of the screw was then compared with peak ratios depending on the formulation used for each run. A low correlation and no significance were found for formulations A and C therefore neither are good predictors for peak ratios. Formulation B presented a negative correlation between those factors ($R^2 = -0.052$) with a significance of $P < 0.05$. The data showed that there is not a correlation between screw speed and peak ratios and is therefore not an adequate predictor. When comparing temperature and peak ratios it was found that the following peaks are

significantly altered ($P < 0.05$): 1366 cm^{-1}, 1434 cm^{-1}, 1555 cm^{-1}, and 1849 cm^{-1} which are all associated with the protein structure except for 1849 cm^{-1}.

3.4 *Effect of extrusion parameters on textural properties*

The formulation of the cereal snack had a significant effect on hardness, brittleness, and crispness after extrusion ($P < 0.05$) (Table 4.4). Hardness and crispness values tended to increase along with the protein to starch ratio whereas brittleness had an indirect relationship dropping from 1.02 to 0.202 mm as seen in Table 4.5. Screw speeds during extrusion had a significant effect on the extrudate responses; the reported values in Table 4.6 display the difference between speeds. For formulations A and B, the hardness values were greatest at screw speeds of 280 RPM.

The change in hardness due to temperature was shown to be significant ($P < 0.05$) on the extrudate similarly to the findings of Ding and others (2006); the values for hardness decreased from 48.07 to 7.77 N (Table 4.7). This is a result of the phase transition of water at high temperatures allowing it to flash off once exiting the die at atmospheric pressure. This flashing off of steam creates numerous air pockets throughout the product and, in turn, decreases the required force to fracture. Temperature also had an effect on the crispness and brittleness of the extrudate with an indirect relationship.

3.5 *Correlation between Raman peak ratios and texture*

Peak ratios of the relative intensity of the Raman peaks were correlated with the texture variables in an effort to determine if there is a predictor of the final properties. The peak ratios occurring at 1366 cm^{-1} for the indole ring of tryptophan and 1434 cm^{-1}, an indicator of C=O

stretch of COO^- in amino acids were significantly ($P < 0.05$), but not highly correlated with hardness ($R^2 = 0.286$), brittleness ($R^2 = 0.222$) and crispness ($R^2 = 0.232$). The intensity of these peaks can be assumed to be directly related to the levels of texture variables. The peak of 1849 cm^{-1}, a C-O stretch of starch, is significantly correlated with hardness ($R^2 = 0.224$) and brittleness ($R^2 = 0.226$). Crispness can also be predicted by the 560 cm^{-1} (pyranose ring) peak whereas another indicator of hardness is at 1555 cm^{-1} (tryptophan).

A regression model was then performed to establish what the best predictors of texture values may be when certain peak ratios are correlated with one another. The results found that 560 cm^{-1}, 1040 cm^{-1}, and 1434 cm^{-1} are marginally important for predicting hardness. These same peaks, along with 1555 cm^{-1}, are the optimal indicators of the level of brittleness in the final product. Peak ratios located at 560 cm^{-1}, 1040 cm^{-1}, 1434 cm^{-1}, and 1849 cm^{-1} provide the most informative conclusions for crispness from Raman.

3.6 *Correlation between non-destructive ultrasound and texture*

Non-destructive ultrasound was used to determine the density of the dough in order to evaluate how that affects the final textural properties. The variable most often used to establish this factor within an ultrasound signal is the attenuation; an example of this signal is shown in Figure 4.5. Attenuation is the degree by which the ultrasonic signal has lost intensity after being sent to the material and reflected back. As the attenuation changes, it exemplifies what is occurring within the dough, whether it is becoming more or less dense in accordance with processing conditions. The results from the non-destructive ultrasound, when taken from three different formulations, three different screw speeds, and various temperature changes, showed a very large range of values with extreme variance. There are significant differences ($P < 0.05$)

from the means of one group of data to the next and also between sets of data. From the results it can be seen that there is significance ($P < 0.05$) between the attenuation and hardness values established from the texture analyzer; this is also the case with brittleness ($P < 0.05$). Unlike the others, the crispness of the cereal snack had no significance ($P > 0.05$) with attenuation. A Pearson correlation was done on the overall texture (compilation of all variables) and the attenuation which resulted in a significant ($P < 0.05$) negative correlation ($R^2 = -0.325$).

4. Conclusion

As extrusion took place, the lipids within the dough were able to withstand high screw speeds and intense shear forces. Amide III, an important indicator of protein structure, was also able to endure screw speeds up to 340 RPM unlike a portion of the starch granules. The phenylalanine band was only present in formulation A even though it contained a lower ratio of protein to starch than B or C. Formulations B and C gave Raman spectra that lacked two identifiable starch bands, 1125 cm^{-1} attributable to C-O-H stretching in amylose and C-O vibration of hydrocarbon chains and 1470 cm^{-1}, a CH_2 bending peak. The appearance of 1290 cm^{-1} only in location C at these formulations indicates both the presence of amylose and amide III. This peak disappeared on the spectra from temperatures above 90°C showing that not all starch and proteins, especially, are able to withstand both extreme heat and shear. The dependence of starch presence on temperature is supported by the lack of 1125 cm^{-1} on all spectra at 100°C or above. Peak ratios calculated from the Raman intensity on the spectra were found to not be adequately predicted by formulation, screw speed, yet were for temperature. Through correlation the peaks located at 560 cm^{-1}, 1040 cm^{-1}, and 1434 cm^{-1} were found to be the best overall indicators of hardness, brittleness, and crispness. In an effort to determine the

effect of density within the extruder on the snack, attenuation was measured and between both hardness and brittleness there was significance with attenuation ($P < 0.05$) but the opposite was the case with crispness ($P > 0.05$).

References

Altomare, R.E., Ghossi, P., 1986. An analysis of residence time distribution patterns in a twin screw cooking extruder. Biotechnology Progress 2, 157-163.

Baeten, V., Hourant, P., Morales, M.T., Aparicio, R., 1998. Oil and fat classification by FT-Raman spectroscopy. Journal of Agricultural and Food Chemistry 46, 2638-2646.

Cael, S.J., Koenig, J.L., Blackwell, J., 1973. Infrared and raman spectroscopy of carbohydrates : Part III: raman spectra of the polymorphic forms of amylose. Carbohydrate Research 29, 123-134.

Collado, L.S., Corke, H., 2003. Characterization of Cereals and Flour. Marcel Dekker, Inc., New York.

Colonna, P., Tayeb, J., Mercier, C., 1989. Extrusion Cooking of Starch and Starchy Products. In C. Mercier, P. Linko, J.M. Harper (Eds.), Extrusion Cooking. American Association of Cereal Chemists, Inc., St. Paul, pp. 247-319.

Ding, Q.-B., Ainsworth, P., Plunkett, A., Tucker, G., Marson, H., 2006. The effect of extrusion conditions on the functional and physical properties of wheat-based expanded snacks. Journal of Food Engineering 73, 142-148.

Ellepola, S.W., Choi, S.M., Phillips, D.L., Ma, C.Y., 2006. Raman spectroscopic study of rice globulin. Journal of Cereal Science 43, 85-93.

Evers, A.D., Blakeney, A.B., L, O., Brien, 1999. Cereal structure and composition. Australian Journal of Agricultural Research 50.

Grenier, P., Bellon-Maurel, V., 2003. Using spectroscopic techniques to monitor food composition. In I.E. Tothill (Ed.), Rapid and on-line instrumentation for food quality assurance. CRC Press LLC, Boca Raton, pp. 291-305.

Hermansson, A.M., Svegmark, K., 1996. Developments in the understanding of starch functionality. Trends in Food Science & Technology 7, 345-353.

Howe, A.M., Mackie, A.R., Robins, M., 1986. Technique to measure emulsion creaming by velocity of ultrasound. Journal of Dispersion Science and Technology 7, 13.

Kizil, R., Irudayaraj, J., Seetharaman, K., 2002. Characterization of irradiated starches by using FT-Raman and FTIR spectroscopy. Journal of Agricultural and Food Chemistry 50, 3912-3918.

Li-Chan, E.C.Y., 1996. The applications of Raman spectroscopy in food science. Trends in Food Science & Technology 7, 361-370.

Martelli, F., 1967. Single- and twin-screw extruders - a technical comparison. Spe Journal 23, 53.

McClements, D.J., 1997. Ultrasonic characterization of foods and drinks: Principles, methods, and applications. Critical Reviews in Food Science and Nutrition 37, 1-46.

Mercier, C., Linko, P., Harper, J.M., 1989. Extrusion Cooking. American Association of Cereal Chemists, Inc. , St. Paul.

Nonaka, M., Lichan, E., Nakai, S., 1993. Raman-spectroscopic study of thermally-induced gelation of whey proteins. Journal of Agricultural and Food Chemistry 41, 1176-1181.

Ozer, E.A., Ibanoglu, S., Ainsworth, P., Yagmur, C., 2004. Expansion characteristics of a nutritious extruded snack food using response surface methodology. European Food Research Technology 218, 6.

Phillips, D.L., Liu, H., Pan, D., Corke, H., 1999. General application of Raman spectroscopy for the determination of level of acetylation in modified starches1. Cereal Chemistry 76, 439-443.

Povey, M.J.W., Harden, C.A., 1981. An application of the ultrasonic pulse echo technique to the measurement of crispness of biscuits. Journal of Food Technology 16, 9.

Smith, E., Dent, G., 2005. Modern Raman Spectroscopy - A Practical Approach. John Wiley & Sons, Ltd, West Sussex, England.

Suetaka, W., Yates, J.T., 1995. Surface Infrared and Raman Spectroscopy: Methods and Applications. Springer, New York.

Tu, A.T., Lee, J., Milanovich, F.P., 1979. Laser-Raman spectroscopic study of cyclohexaamylose and related compounds; spectral analysis and structural implications. Carbohydrate Research 76, 6.

Tuma, R., 2005. Raman spectroscopy of proteins: from peptides to large assemblies. Journal of Raman Spectroscopy 36, 307-319.

Vasko, P.D., Blackwell, J., Koenig, J.L., 1971. Infrared and raman spectroscopy of carbohydrates : Part I: Identification of O---H and C---H-related vibrational modes for D-glucose, maltose, cellobiose, and dextran by deuterium-substitution methods. Carbohydrate Research 19, 297-310.

Table 4.1: Ingredient formulations used during the extrusion of a cereal snack on a 3.632 kg basis (Ozer et al. 2004)

Formulation	Chickpea Flour (kg)	Corn Flour (kg)	Oat Flour (kg)	Cornstarch (kg)	Tomato Powder (kg)	Ground Raw Hazelnuts (kg)
A	1.0896	.7264	.7264	.5448	.3632	.1816
B	1.2712	.7264	.7264	.3632	.3632	.1816
C	1.4528	.7264	.7264	.1816	.3632	.1816

Table 4.2: Independent extrusion parameters utilized to control processing

Formulation	Batch	Feeder Speed (RPM)	Barrel Temp* (°C)	Screw Speed (RPM)	Drying Time (Hrs)
A	1	300	90	220	8
	2	300	90	280	8
	3	300	90	340	8
	4	300	90	280	5
	5	300	100	280	5
	6	300	110	280	5.5
	7	300	120	280	5
	8	300	90, 100, 110	280	5
B	1	295	90	220	9
	2	295	90	280	9
	3	295	90	340	9
C	1	300	90	220	5
	2	300	90	280	5
	3	300	90	340	5

*Actual temperatures were ±2°C

Table 4.3. Raman band identification useful for cereal-based products

Wavenumber (cm^{-1})	Origin	Band assignment
480	starch	C-H stretch
500 – 540	cysteine, cystine	S-S stretch
560	starch	pyranose ring
600		phenylalanine
670	cysteine	C-S stretching
700 – 745	cysteine	C-S stretching
830 – 850	tyrosine	phenol group
	hydrocarbon chains	C - O
1040	amylose	C-O-H bending
1130	starch	C-O stretching,
		C-O-H bending
	hydrocarbon chains	C-O vibration
1260 – 1290	amylose	CH_2OH side chain
	amide III	N-H bend,
		C-N stretch
1360	tryptophan	indole ring
1430	aspartic & glutamic acids	C=O stretch of COO^-
1460	starch	CH_2 bending
1500	lipids	CH_2 scissoring
1555		tryptophan
1570	amide II	C-N stretching
1640	lipids	C=C stretching
1655	lipids	C=C stretching
	amide I	amide C=O stretch
1849	starch	C-O stretching

[a]Adapted from Baeten et al. (1998), Cael et al. (1973), Ellepola et al. (2006), Kizil et al. (2002), Li-Chan et al. (1996), Nonaka et al. (1993), Phillips et al. (1999), Tuma (2005), Vasko et al. (1971), Suetaka et al. (1995)

Table 4.4. ANOVA of extrudate responses

Parameter	Hardness	Brittleness	Crispness
Formulation	**	**	**
Screw Speed	**	**	**
Temperature	**	**	**

** indicates significance at P-value < 0.05

Table 4.5. Mean data of texture responses to formulation changes

Formulation	**Hardness (N)**	**Brittleness (mm)**	**Crispness (mm^{-1})**
A	29.23^{a}	1.02^{a}	27.29^{a}
B	23.69^{a}	0.75^{b}	25.77^{a}
C	1.16^{b}	0.20^{c}	5.25^{b}

Means with the same letter in each column are not significantly different ($P > 0.05$)

Table 4.6. Mean data of texture responses to screw speed changes

Speed (RPM)	**Hardness (N)**	**Brittleness (mm)**	**Crispness (mm^{-1})**
220	15.84^{a}	0.58^{b}	19.27^{ab}
280	24.84^{b}	0.80^{a}	22.87^{a}
340	16.88^{a}	0.53^{b}	16.18^{b}

Means with the same letter in each column are not significantly different ($P > 0.05$)

Table 4.7. Mean data of texture responses to temperature changes

Temperature (°C)	**Hardness (N)**	**Brittleness (mm)**	**Crispness (mm^{-1})**
90	48.07^{a}	1.32^{a}	37.65^{a}
100	49.14^{a}	1.39^{a}	36.66^{ab}
110	23.30^{b}	0.66^{b}	30.71^{b}
120	8.77^{c}	0.50^{b}	18.43^{c}
90,100, 110	7.77^{c}	0.39^{b}	17.81^{c}

Means with the same letter in each column are not significantly different ($P > 0.05$)

Table 4.8. Peak ratios of prominent Raman bands as used for analysis of a cereal-based product

Form	Speed	Loc	Rep	480 cm^{-1}	500-540 cm^{-1}	1040 cm^{-1}	1360 cm^{-1}	1430 cm^{-1}	1555 cm^{-1}	1849 cm^{-1}
A	220	A	1	0.03779	0.08555	0.36524	1.60987	1.58606	1.57766	0.55765
A	220	A	2	0.11076	0.12249	0.38344	1.52992	1.50142	1.47936	0.40896
A	220	A	3	0.18888	0.28041	0.56004	1.57341	1.52501	1.46457	0.61038
A	220	B	1	0.10678	0.11365	0.40235	1.54038	1.52227	1.47426	0.54446
A	220	B	2	0.11489	0.08748	0.40989	1.60669	1.55219	1.57986	0.56205
A	220	B	3	0.11163	0.17551	0.40924	1.60098	1.58306	1.51714	0.47735
A	220	C	1	0.02735	0.03632	0.35810	1.66319	1.62949	1.61600	0.54265
A	220	C	2	0.02445	0.04017	0.36746	1.70793	1.66308	1.64138	0.58206
A	220	C	3	0.21062	0.36137	0.56621	1.44300	1.39278	1.35494	0.56439
A	280	A	1	0.04289	0.03455	0.39020	1.63125	1.60764	1.59405	0.56799
A	280	A	2	0.13689	0.17940	0.36147	1.56303	1.56836	1.55121	0.55828
A	280	A	3	0.11671	0.35876	0.58093	1.61741	1.61943	1.52996	0.68103
A	280	B	1	0.08451	0.12414	0.40822	1.53197	1.52908	1.48703	0.55642
A	280	B	2	0.10663	0.11149	0.42095	1.58122	1.55568	1.52887	0.58329
A	280	B	3	0.13151	0.14919	0.38232	1.53259	1.49915	1.46105	0.50114
A	280	C	1	0.17401	0.08148	0.40535	1.60819	1.58995	1.55583	0.54724
A	280	C	2	0.12812	0.10520	0.38466	1.48941	1.51043	1.47726	0.50257
A	280	C	3	0.10897	0.11513	0.38793	1.50858	1.51043	1.47726	0.51220
A	340	A	1	0.08795	0.08589	0.35008	1.55573	1.53221	1.50611	0.54713
A	340	A	2	0.12927	0.13283	0.39259	1.52390	1.47764	1.45524	0.51393
A	340	A	3	0.15969	0.26387	0.54851	1.56474	1.56259	1.51445	0.62926
A	340	B	1	0.09661	0.10338	0.40457	1.59364	1.53221	1.50727	0.57234
A	340	B	2	0.15136	0.10338	0.36984	1.54222	1.54665	1.49447	0.54408

Form	Speed	Loc	Rep	480 cm^{-1}	500-540 cm^{-1}	1040 cm^{-1}	1360 cm^{-1}	1430 cm^{-1}	1555 cm^{-1}	1849 cm^{-1}
A	340	B	3	0.12209	0.11802	0.39601	1.58633	1.55947	1.54493	0.52584
A	340	C	1	0.11974	0.11619	0.41887	1.52687	1.51621	1.48864	0.52637
A	340	C	2	0.14277	0.14131	0.38352	1.50884	1.52405	1.48485	0.53469
A	340	C	3	0.11871	0.11515	0.35057	1.54736	1.52598	1.50382	0.51882
B	220	A	1							
B	220	A	2	0.13739	0.15458	0.32506	1.61017	1.56449	1.52835	0.51628
B	220	A	3	0.10619	0.13555	0.37626	1.62128	1.58042	1.55706	0.54470
B	220	B	1							
B	220	B	2	0.12128	0.13970	0.39069	1.59767	1.55949	1.55359	0.55305
B	220	B	3	0.16585	0.14448	0.42388	1.53608	1.52379	1.47872	0.54052
B	220	C	1	0.09516	0.14281	0.36724	1.57216	1.54445	1.53201	0.51675
B	220	C	2	0.12821	0.15947	0.39783	1.59647	1.54634	1.49604	0.52179
B	220	C	3	0.11825	0.14244	0.38556	1.54216	1.51965	1.51294	0.52483
B	280	A	1							
B	280	A	2	0.07261	0.07381	0.40281	1.59342	1.59247	1.57747	0.56438
B	280	A	3	0.10887	0.11894	0.41385	1.61288	1.56587	1.57147	0.59333
B	280	B	1							
B	280	B	2	0.03738	0.06335	0.38438	1.62761	1.62215	1.62629	0.54522
B	280	B	3	0.11138	0.06335	0.39774	1.55618	1.52065	1.51409	0.50512
B	280	C	1							
B	280	C	2	0.12303	0.11241	0.43393	1.5579	1.5236	1.50832	0.51908
B	280	C	3	0.10316	0.20914	0.40129	1.51791	1.5002	1.44974	0.50829
B	340	A	1	0.12859	0.14067	0.39081	1.55918	1.54336	1.54398	0.55095
B	340	A	2	0.09254	0.14889	0.34853	1.63574	1.61874	1.67742	0.57463

Form	Speed	Loc	Rep	480 cm^{-1}	500-540 cm^{-1}	1040 cm^{-1}	1360 cm^{-1}	1430 cm^{-1}	1555 cm^{-1}	1849 cm^{-1}
B	340	A	3	0.10427	0.12791	0.35795	1.59325	1.55497	1.58095	0.54294
B	340	B	1	0.09655	0.10605	0.41019	1.55350	1.54330	1.51701	0.52909
B	340	B	2	0.12834	0.10605	0.38613	1.59101	1.58069	1.51548	0.54974
B	340	B	3	0.14196	0.11033	0.40560	1.56866	1.54572	1.55669	0.52618
B	340	C	1	0.10623	0.12261	0.41236	1.55564	1.51218	1.48678	0.48213
B	340	C	2	0.14509	0.23282	0.38294	1.47407	1.44937	1.45099	0.48162
B	340	C	3	0.12294	0.14983	0.42014	1.58632	1.54219	1.52516	0.56028
C	220	A	1	0.13158	0.12033	0.36756	1.61461	1.59841	1.63143	0.56210
C	220	A	2	0.10273	0.11402	0.38446	1.58001	1.56294	1.58560	0.54858
C	220	A	3	0.10192	0.13402	0.30164	1.63844	1.58348	1.61349	0.53692
C	220	B	1	0.11569	0.13893	0.40315	1.61153	1.55443	1.56958	0.54762
C	220	B	2	0.07423	0.13893	0.41081	1.58311	1.51601	1.50687	0.54026
C	220	B	3	0.11490	0.16634	0.40215	1.54342	1.52201	1.53229	0.55344
C	220	C	1	0.13938	0.12417	0.38951	1.56163	1.53279	1.50951	0.53109
C	220	C	2	0.15466	0.32341	0.48253	1.47577	1.43709	1.40068	0.50765
C	220	C	3	0.25289	0.40696	0.41379	1.45018	1.41975	1.40097	0.45675
C	280	A	1	0.10783	0.13709	0.31443	1.52223	1.55981	1.59131	0.52965
C	280	A	2	0.09256	0.07556	0.28717	1.59845	1.57341	1.59044	0.54045
C	280	A	3	0.12455	0.13899	0.29441	1.54845	1.56315	1.56059	0.54237
C	280	B	1	0.05703	0.07815	0.41205	1.62014	1.58916	1.53723	0.56159
C	280	B	2	0.05719	0.06821	0.36848	1.53123	1.54774	1.52897	0.55653
C	280	B	3	0.13816	0.13764	0.40524	1.54857	1.50774	1.51519	0.54203
C	280	C	1	0.12408	0.18863	0.38519	1.55423	1.51556	1.52259	0.50373
C	280	C	2	0.05345	0.05206	0.36303	1.57891	1.55963	1.54414	0.56674

Form	Speed	Loc	Rep	480 cm^{-1}	500-540 cm^{-1}	1040 cm^{-1}	1360 cm^{-1}	1430 cm^{-1}	1555 cm^{-1}	1849 cm^{-1}
C	280	C	3	0.13682	0.180347	0.42198	1.52859	1.51305	1.51231	0.53176
C	340	A	1	0.14069	0.14117	0.36152	1.56524	1.53475	1.57029	0.53989
C	340	A	2	0.11707	0.15538	0.35606	1.57098	1.53096	1.59890	0.54532
C	340	A	3	0.13487	0.12984	0.35804	1.57114	1.55656	1.56351	0.52018
C	340	B	1	0.11302	0.12528	0.39252	1.52836	1.49748	1.47269	0.51438
C	340	B	2	0.13021	0.13678	0.41938	1.56937	1.52442	1.54688	0.53890
C	340	B	3	0.13478	0.11065	0.41232	1.55099	1.50764	1.52954	0.58328
C	340	C	1	0.11800	0.11214	0.41575	1.53593	1.48784	1.52595	0.51598
C	340	C	2	0.12860	0.14453	0.43140	1.52424	1.51144	1.48701	0.53622
C	340	C	3	0.13295	0.13788	0.42461	1.52406	1.49836	1.50176	0.54166

Form	Temp	Loc	Rep	480 cm^{-1}	500-540 cm^{-1}	1040 cm^{-1}	1360 cm^{-1}	1430 cm^{-1}	1555 cm^{-1}	1849 cm^{-1}
A	90	A	1	0.09602	0.09963	0.37632	1.60801	1.58551	1.61344	0.54727
A	90	A	2	0.08099	0.10263	0.32364	1.61507	1.59644	1.62755	0.54428
A	90	A	3	0.11262	0.09703	0.33732	1.63379	1.62499	1.64009	0.55558
A	90	B	1	0.07886	0.08729	0.42155	1.57133	1.55581	1.59709	0.55806
A	90	B	2	0.08124	0.07729	0.38934	1.62564	1.60807	1.64513	0.55650
A	90	B	3	0.07491	0.08887	0.36686	1.60560	1.58085	1.61514	0.54925
A	90	C	1	0.13309	0.14546	0.41882	1.56331	1.53240	1.53964	0.54475
A	90	C	2	0.07339	0.10954	0.40157	1.61819	1.58489	1.59363	0.56759
A	90	C	3	0.12155	0.08935	0.40572	1.58091	1.53049	1.55914	0.52749
A	100	A	1	0.10031	0.13704	0.33658	1.59517	1.52744	1.57132	0.55752
A	100	A	2	0.11563	0.13428	0.39327	1.53453	1.54862	1.54726	0.55616
A	100	A	3	0.14559	0.11824	0.33832	1.55537	1.52204	1.58275	0.55423

Form	Temp	Loc	Rep	480 cm^{-1}	500-540 cm^{-1}	1040 cm^{-1}	1360 cm^{-1}	1430 cm^{-1}	1555 cm^{-1}	1849 cm^{-1}
A	100	B	1	0.10281	0.12328	0.39625	1.50769	1.54464	1.52817	0.54304
A	100	B	2	0.06350	0.07635	0.37824	1.62978	1.58091	1.59159	0.53497
A	100	B	3	0.05926	0.07938	0.40448	1.59628	1.56725	1.55405	0.54261
A	100	C	1	0.13613	0.14149	0.42872	1.60357	1.60021	1.58779	0.54618
A	100	C	2	0.13637	0.14616	0.44569	1.59601	1.58561	1.52069	0.57877
A	100	C	3	0.11812	0.10993	0.40882	1.57796	1.54666	1.50549	0.54251
A	110	A	1	0.05354	0.07590	0.32188	1.60434	1.47749	1.58946	0.56843
A	110	A	2	0.05658	0.08404	0.29603	1.55199	1.51102	1.53673	0.48995
A	110	A	3	0.14550	0.14293	0.35152	1.54105	1.50233	1.45261	0.49563
A	110	B	1	0.14886	0.13940	0.41901	1.60491	1.55329	1.50742	0.51128
A	110	B	2	0.11272	0.13149	0.39592	1.58626	1.54112	1.56347	0.55656
A	110	B	3	0.12053	0.12233	0.41206	1.55301	1.50678	1.55052	0.50708
A	110	C	1	0.10999	0.12576	0.39724	1.58464	1.54366	1.53627	0.50952
A	110	C	2	0.06695	0.05656	0.36953	1.53205	1.53506	1.56382	0.51925
A	110	C	3	0.13385	0.14034	0.40708	1.54171	1.48327	1.47455	0.49843
A	120	A	1	0.09890	0.09905	0.31209	1.59005	1.56529	1.62193	0.53725
A	120	A	2	0.14194	0.14248	0.31296	1.51476	1.49846	1.52490	0.51373
A	120	A	3	0.14346	0.16419	0.33439	1.54427	1.49609	1.53905	0.51104
A	120	B	1	0.09993	0.11809	0.40436	1.53888	1.49608	1.47254	0.48411
A	120	B	2	0.11848	0.13047	0.40312	1.54726	1.50592	1.49099	0.55100
A	120	B	3	0.04808	0.05416	0.37517	1.54028	1.52187	1.53476	0.51294
A	120	C	1	0.09951	0.13169	0.33221	1.42120	1.36790	1.37623	0.44156
A	120	C	2	0.16877	0.16076	0.39044	1.48218	1.44666	1.43315	0.51013
A	120	C	3	0.10408	0.11642	0.35856	1.49381	1.47533	1.48517	0.49020

Form	Temp	Loc	Rep	480 cm^{-1}	500-540 cm^{-1}	1040 cm^{-1}	1360 cm^{-1}	1430 cm^{-1}	1555 cm^{-1}	1849 cm^{-1}
A	90,100,110	A	1	0.12376	0.13939	0.38844	1.58596	1.54958	1.58412	0.53191
A	90,100,110	A	2	0.15660	0.16006	0.30626	1.57263	1.55659	1.58353	0.55025
A	90,100,110	A	3	0.10501	0.10849	0.29875	1.61113	1.55547	1.61278	0.52296
A	90,100,110	B	1	0.10183	0.09504	0.41549	1.62917	1.61561	1.59116	0.59629
A	90,100,110	B	2	0.113791	0.11352	0.41228	1.56085	1.53449	1.52132	0.51454
A	90,100,110	B	3	0.12098	0.13093	0.39689	1.53706	1.51522	1.49527	0.49346
A	90,100,110	C	1	0.10591	0.09908	0.35962	1.56679	1.53019	1.51313	0.53457
A	90,100,110	C	2	0.12005	0.11019	0.35680	1.49585	1.46894	1.45495	0.47065
A	90,100,110	C	3	0.12253	0.12211	0.38873	1.55422	1.48956	1.52849	0.51075

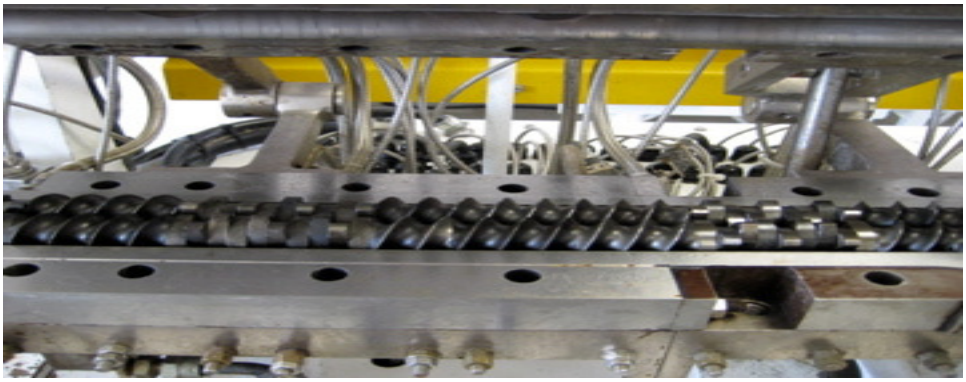

Figure 4.1: Twin-screw, co-rotating, intermeshing extruder configuration

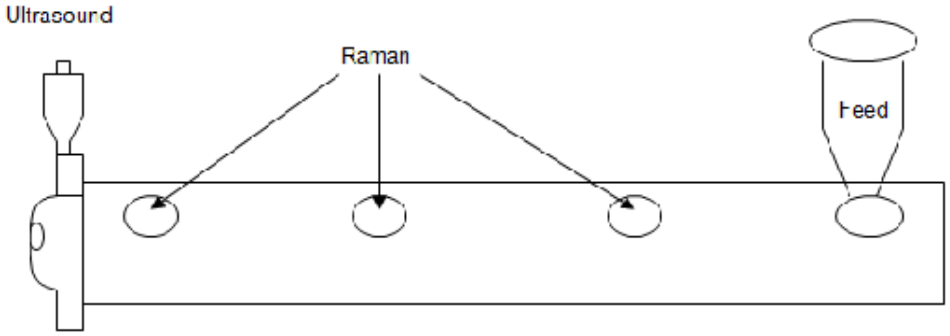

Figure 4.2: On-line monitoring setup of a Raman spectrometer and non-destructive ultrasound device during extrusion

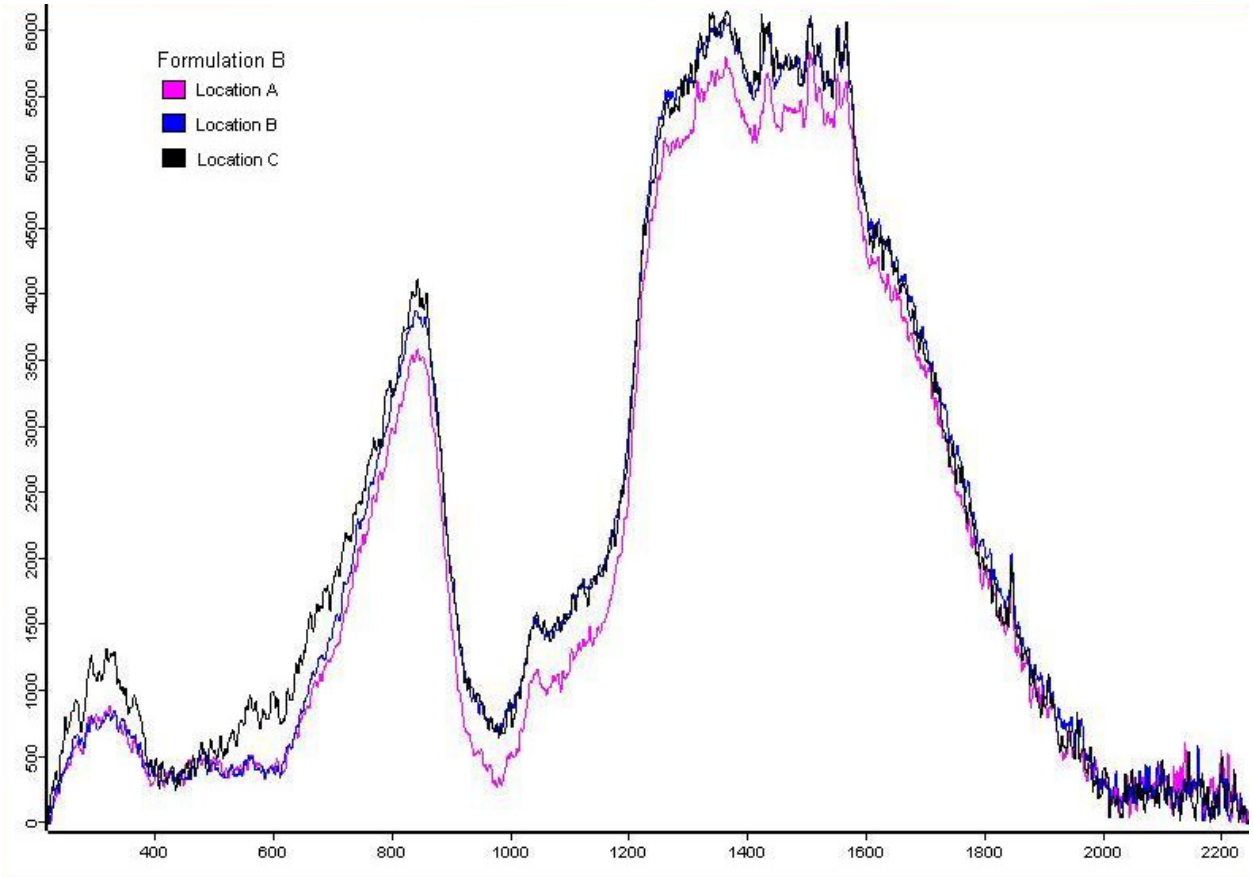

Figure 4.3. Raman spectra of formulation B at locations 1, 2, and 3 throughout the extruder

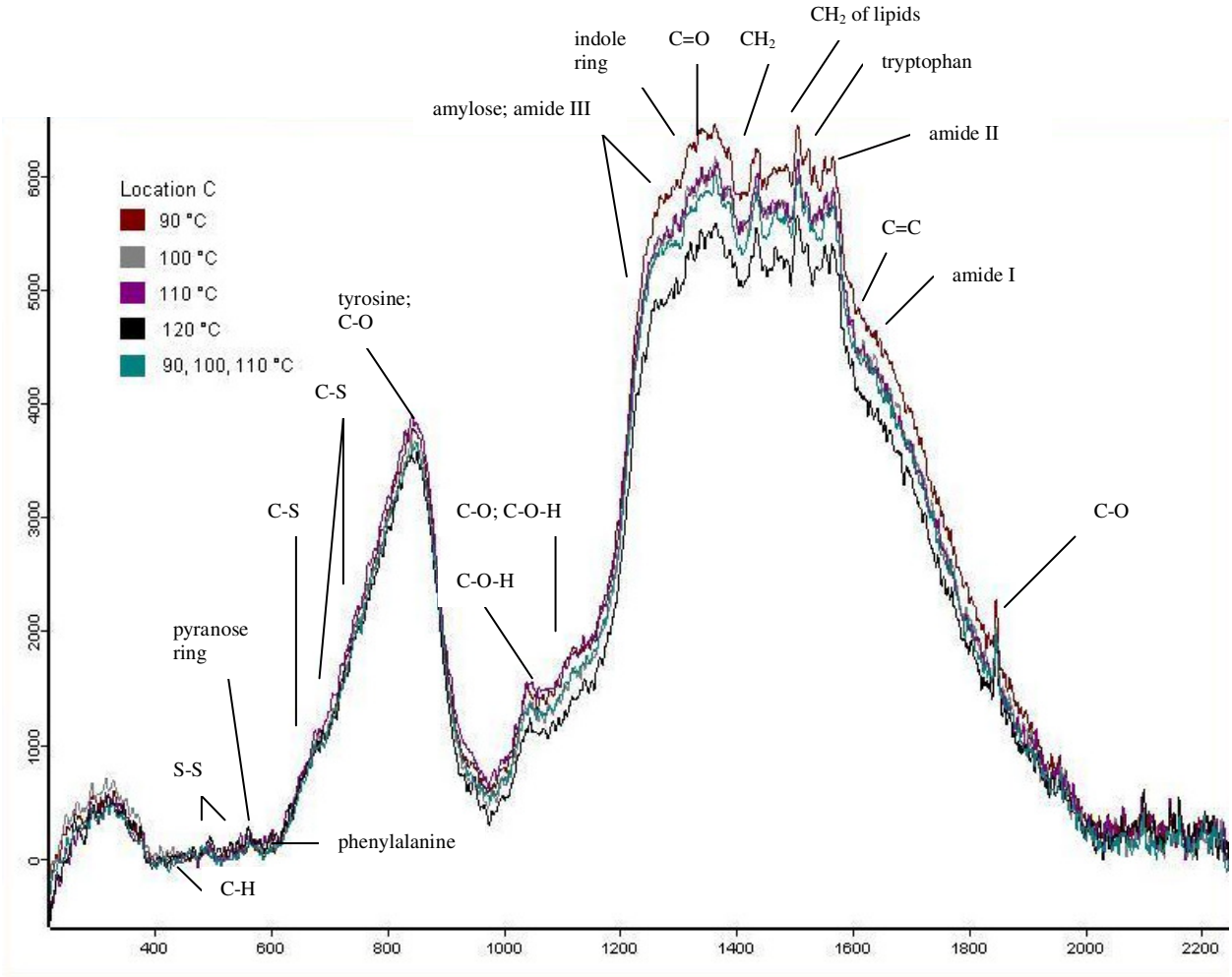

Figure 4.4. Raman spectra of temperature changes at location 1 in the extruder

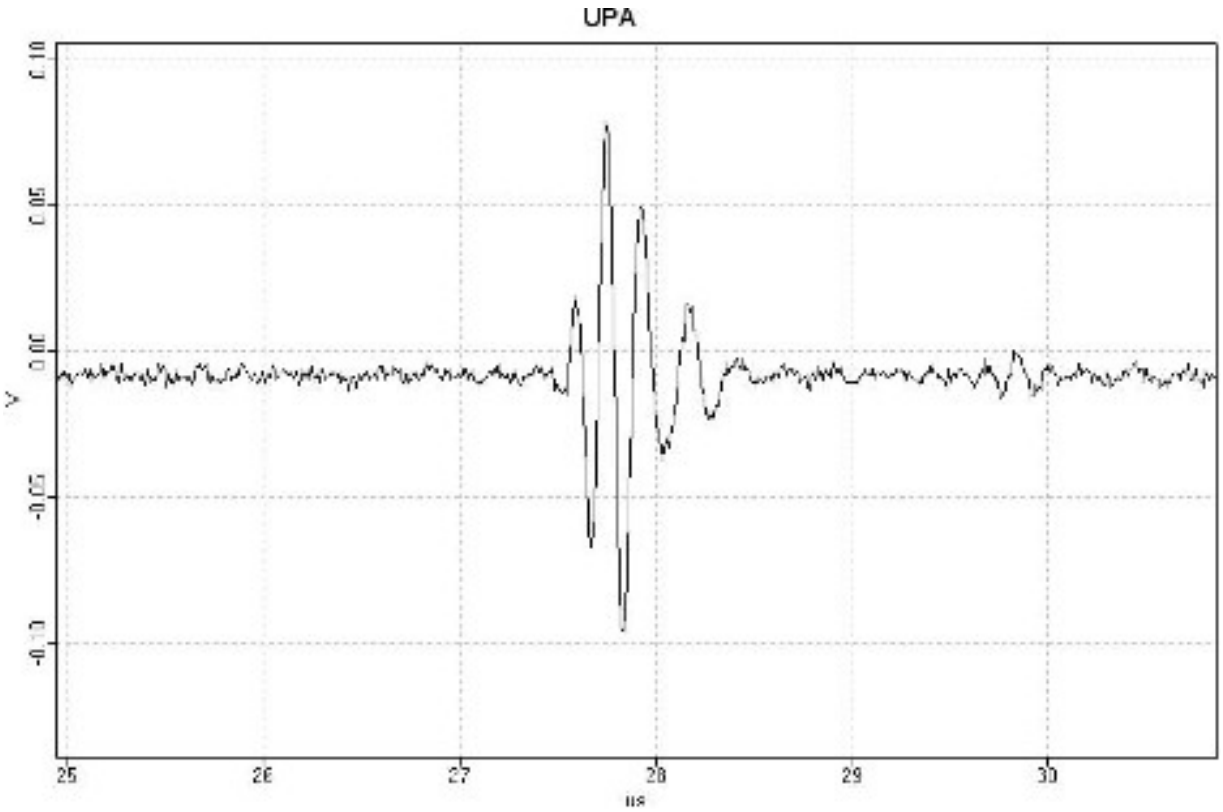

Figure 4.5. Ultrasonic signal during extrusion of cereal-based snack

CHAPTER 5

CONCLUSIONS

The data in chapter 3 shows that independent extrusion variables produced significant changes within cereal-based snacks. Temperature had the greatest affect on texture, color, and expansion properties due to the heightened air incorporation once the product exited the die; production formulation and screw speed also produced significant differences in the extrudate's physical properties and can be adjusted according to the desired outcome. The negative correlation between textural variables and L^* and b^* indicate that the product will become lighter as the amount of force and distance required to fracture the extrudate decreases.

Chapter 4 describes the utilization of on-line monitoring devices during extrusion to determine the type of bonding characteristics that take place. As extrusion was performed the lipids within the dough were able to withstand high screw speeds and intense shear forces. Amide III, an important indicator of protein structure, was also able to endure screw speeds up to 340 RPM unlike a portion of the starch granules. The phenylalanine band was only present in formulation A even though it contained a lower ratio of protein to starch than B or C. Formulations B and C gave Raman spectra that lacked two identifiable starch bands, 1125 cm^{-1} attributable to C-O-H stretching in amylose and C-O vibration of hydrocarbon chains and 1470 cm^{-1}, a CH_2 bending peak. The appearance of 1290 cm^{-1} only in location C at these formulations indicates both the presence of amylose and amide III. This peak disappeared on the spectra from temperatures above 90°C showing that not all starch and proteins, especially, are able to withstand both extreme heat and shear. The dependence of starch bonding on temperature is supported by the lack of 1125 cm^{-1} on all spectra at 100°C or above. Peak ratios calculated from the Raman intensity on the spectra were found to not be adequately predicted by formulation,

screw speed, yet were for temperature. Through correlation the peaks located at 560 cm^{-1}, 1040 cm^{-1}, and 1434 cm^{-1} were found to be the best overall indicators of hardness, brittleness, and crispness. In an effort to determine the effect of density within the extruder on the snack, attenuation was measured with a non-destructive ultrasound device and between both hardness and brittleness there was significance with attenuation ($P < 0.05$) but the opposite was the case with crispness ($P > 0.05$).